Table 1
Characteristics of the study populations and association analysis of the G664A polymorphism in relation to cerebral infarction

	First panel			Second panel		
	Cases		Controls	Symptomatic subcortical infarction	Silent brain infarction	Controls
No. of subjects (M/F)	270 (127/143)		359 (170/189)	74 (51/23)	104 (62/42)	163 (97/66)
Age (years)	69.5±7.8		68.6±6.4	65.8±10.7*	69.4±9.8*	57.0±7.9
Hypertension (%)	60		57	82*	69*	18
Diabetes (%)	22*		13	28*	12	11
Hypercholesterolemia (%)	57		59	34	52*	37
Smoking (%)	38		34	41	39	34
Genotype distribution for the G664A polymorphism	Total cases	(Subjects with subcortical infarction)				
G/G	230 (85%)	(104 (85%))	298 (83%)	64 (86%)	88 (85%)	127 (78%)
G/A	37 (14%)	(16 (13%))	58 (16%)	10 (14%)	14 (13%)	35 (21%)
A/A	3 (1%)	(3 (2%))	3 (1%)	0 (0%)	2 (2%)	1 (1%)
Frequency of 664A allele	8.0%	(8.9%)	8.9%	6.8%	8.7%	11.3%

In the original report by Rubattu et al. [8], the 664A allele was assumed to confer an increased risk for stroke. First and second panels were collected independently, according to classification criteria previously described in detail [10,11]. Cases in the first panel comprised patients with focal neurological symptoms due to cerebral infarction and excluded those with intracerebral or subarachnoid hemorrhage or those with cardiovascular complications, such as atrial fibrillation, vasculitis and a history of cardiac surgery. Controls in the first panel were ascertained from the same area with the frequencies of age and sex being matched. In the second panel, all subjects were evaluated by MRI; 104 subjects with silent brain infarction and 163 with cerebral infarctions (control group) were selected from people undergoing a health screening examination, while 74 patients with symptomatic subcortical infarction were also included in the study. Classification criteria for confounding factors were as follows: Hypertension was defined by either (1) BP measurements exceeded systolic BP ≧ 160 mmHg and/or diastolic BP ≧ 95 mmHg on two consecutive visits for untreated subjects or (2) chronic antihypertensive treatment of patients. Diabetes mellitus was defined by either (1) fasting plasma glucose concentration ≧ 7.7 mmol/l and/or a diabetic pattern was observed after an oral glucose challenge or (2) those under chronic treatment with oral hypoglycemic agents or insulin. Hypercholesterolemia was defined by either (1) serum cholesterol levels ≧ 5.70mmol/l for those untreated or (2) patients receiving cholesterol-lowering drugs.

* $P < 0.05$ versus controls by t-test of χ^2-test.

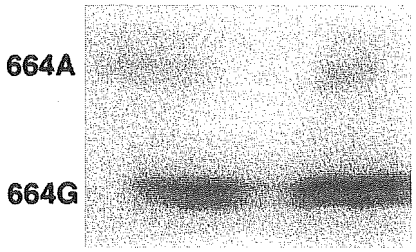

Fig. 1. A G664A polymorphism used for genotyping in the case-control analysis. After MS-PCR, the products were electrophoresed in 6% polyacrylamide/7 M urea gels and transferred to nylon membranes. The membranes were then hybridized with a ^{32}P-labeled primer and subjected to autoradiography.

and SHRSP as a whole hereafter. Ten SHR substrains derived from three colonies were used for DNA analysis in the present study. These included: three SHRSP (A_{1-sb}, A_3 and A_4) and four SHRSR (B_1, B_2, CH and CL) substrains from a colony kept at Kyoto University, Kyoto, Japan (SHRSP/Izm and SHRSR/Izm), SHRSP and SHRSR from the Max Delbruck Center for Molecular Medicine in Berlin-Buch, Germany (SHRSP/Heidelberg and SHRSR/Heidelberg) and SHRSR from the Genetic Resource Section, the National Institute of Health, Bethesda (SHRSR/NIH). The WKY rat from a colony kept at our institution (WKY/Izm) was used as a normotensive control strain. The genealogy of SHR substrains was described elsewhere [2,3,15,16]. Briefly, selective breeding was originally made for stroke-proneness to separate SHRSP from the *A* subline of SHR during F_{24-25} generations (in 1971), by which time three distinct sublines of SHR (the *A–C* sublines) had been maintained in Kyoto. Stroke-resistant SHR, SHRSR, was thereafter derived from the *B* and *C* sublines and seven substrains of SHR (three SHRSP and four SHRSR substrains) have been kept at our institution, all direct descendants of the original colony. SHRSR/NIH was separated from a Japanese colony as early as F_{13} generation and established as an inbred strain at the NIH. SHRSP/Heidelberg was separated from the A_3 substrain of SHRSP/Izm at F_{36} generation (in 1975), but we do not know the details of the origin of SHRSR/Heidelberg. Two SHR substrains of a Japanese colony, descendants of SHRSP (A_3) and SHRSR (B_1), were further investigated in the gene expression study. For this purpose, animals were fed on a regular rat chow diet and sacrificed under pentobarbital anesthesia at 13 weeks of age. All procedures were in accordance with institutional guidelines.

2.4. Sequence comparison of rat ANP among substrains of SHRSP and SHRSR and WKY/Izm

Genomic ANP fragments, 2170-bp in size, were sequenced and compared among seven SHR substrains of a Japanese colony and WKY/Izm. Additionally, a 408-bp fragment spanning from intron 1 to intron 2 was sequenced for SHRSP/Heidelberg, SHRSR/Heidelberg, and SHRSR/NIH. Five overlapping sets of PCR primers were designed to cover a 625-bp 5′-untranslated region (UTR), three exons and two introns and a 591-bp 3′UTR in the rat ANP gene (Fig. 2). After PCR amplification, the products were gel-purified and subjected to cycle-sequencing according to the manufacturer's protocol (Dye-Terminator Cycle sequencing kit) on an ABI 377 DNA sequencer (Applied Biosystems). Information of the PCR primers can be obtained from the authors upon request.

2.5. Substrain comparison of marker alleles on rat chromosome 5

In the region which was assumed to encompass QTLs for 'stroke-associated' phenotypes on rat chromosome 5 [5,6], we examined allele distribution patterns of microsatellite markers among ten substrains of SHR and WKY/Izm. Substrain comparison was made by scoring 42 markers, where the allele size of PCR products was determined in base pair on an ABI 377 DNA Sequencer (Applied Biosystems).

A genetic linkage map of the relevant chromosomal region was constructed by genotyping all informative markers on 110 male F_2 rats involving the A_3 substrain of SHRSP/Izm and WKY/Izm to complete our consensus map. Genotyping and linkage mapping were performed as previously described [17].

As for the ANP locus, to differentiate base substitutions identified in intron 2 of the gene, a set of MS-PCR primers were newly designed as follows:

FP, 5′-AGGATCTGAGCCACGAGCAC-3′
RP-WKY, 5′-TCCCACCAGCCACAGTCTG-3′
RP-SP, 5′-CCAGTGACCAAGTCTTAGCCACCAGC CACAGTCCA-3′
where deliberate differences and base substitutions are underlined [18].

2.6. Gene expression studies

Total RNA was extracted from the whole brain of SHRSP/Izm and SHRSR/Izm for Northern blotting. A semi-quantitative PCR assay was also performed using the full-length cDNAs synthesized from reverse-transcribed mRNA of the brain. The PCR primers were: 5′TCTGATGGATTTCAAGAACCTG3′ (forward) and 5′TCAATCCTACCCC-CGAAGCAG3′ (reverse), where a forward primer was designed to be located on separate exons (exons 1 and 2) in order to eliminate PCR amplification from contaminating genomic DNA. PCR was terminated during the exponential phase and the products were electrophoresed on a 2% agarose gel. Quantitative analysis was performed by densitometric scanning on an AlphaImager 2000 (Alpha Innotech) and normalized by GAPDH levels.

3. Results

3.1. Association of G664A with human stroke

Table 1 shows baseline characteristics in our study panels. Apart from the status of diabetes mellitus, five variables—sex, age, and the status of hypertension, hypercholesterolemia and smoking—were comparable between case and control groups in the first panel. On the other hand, some variables were not comparable among three groups in the second panel, which was inevitable due to the consecutive enrollment scheme. Genotype characterization of the G664A polymorphism was performed by MS-PCR (Fig. 1) and no significant association was seen between case and control groups in either of panels. The results were almost unchanged when each study group was stratified by the presence or absence of hypertension and when confounding factors

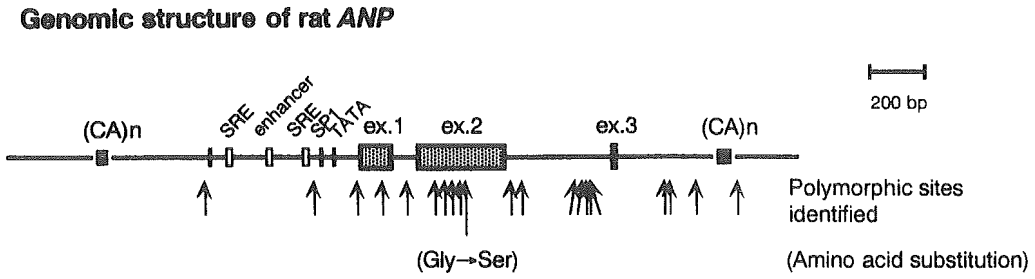

Fig. 2. Sequence differences identified between SP/Izm-type and WKY/Izm-type alleles of the rat ANP gene. Two distinct alleles were inferred from the 21 polymorphic sites identified in the sequenced region. Only a G-to-A substitution at position 485 from the CAP site resulted in an amino acid change, Gly-to-Ser, at residue 100 of prepro-ANP. SRE, serum response element; SP-1, promoter-specific transcription factor.

were adjusted by a multivariate analysis (data not shown). Restricting to patients with subcortical infarction did not influence the results for association. While no significant association was observed between C-664G and T1766C and stroke status, rarer allele frequencies did not exceed 3% in the Japanese population for either of two polymorphisms. This precluded haplotype analysis (data not shown). The prevalence of tested polymorphisms in each study group was consistent with Hardy–Weinberg equilibrium.

3.2. Sequence analysis of rat ANP

A total of 21 base-substitution polymorphisms were identified by direct sequencing of the rat ANP gene (Fig. 2). While six polymorphisms were located in exons, only a G-to-A substitution at position 485 from the CAP site (which was previously numbered as 1125 according to the deposited sequences, K02062 and K02063) [7] resulted in an amino acid change, Gly-to-Ser, at residue 100 of prepro-ANP. In a region of 625-bp upstream of the CAP site, we found three polymorphisms: G-to-T at position −463, C-to-T at position −88, and C-to-T at position 86. Here, a G-to-T substitution at position −463 was localized on the putative PEA-2 polyoma enhancer binding site [19] and a C-to-T substitution at position 86 was 1-bp upstream of the ATG starting codon [20]; these are considered functionally important. Two of the polymorphisms (a G-to-A substitution at position 485 and a G-to-T substitution at position −463) had been shown in a Heidelberg colony [7].

Two distinct types of ANP alleles were inferred from 21 polymorphic sites in the sequenced region. In a Japanese colony, all three SHRSP substrains possessed an identical allele (SP/Izm-type), while four SHRSR substrains and WKY/Izm shared the other allele (WKY/Izm-type). In addition, sequencing of a 408-bp genomic fragment, where six polymorphisms had been detected, revealed that SHRSP/Heidelberg possessed a SP/Izm-type allele, while SHRSR/Heidelberg and SHRSR/NIH possessed a WKY/Izm-type allele (Fig. 3). Judging from four exon 2 polymorphisms reported by Brosnan et al. [9], SHRSP/Glasgow and WKY of a Glasgow colony (WKY/Glasgow) were thought to possess a SP/Izm-type allele.

3.3. Allele distribution patterns on rat chromosome 5

To explore the relevance of substrain differences to 'stroke-associated' QTLs on rat chromosome 5, we determined allele distribution patterns of 42 microsatellite markers among ten substrains of SHR and WKY/Izm (Fig. 3). A small interval (< 10 cM in size) flanked by D5Mit11 and D5Rat24 differed between three SHRSP and four SHRSR substrains of a Japanese colony, whereas allele distribution patterns in the corresponding region were identical among two substrains of a Heidelberg colony and SHRSR/NIH. By contrast, the type of alleles at two adjacent loci, D5Mgh15 and ANP, differed between SHRSP and SHRSR substrains regardless of the origin of colonies.

3.4. Rat ANP gene expression

We found no detectable ANP mRNA expression of the rat brain by Northern blot analysis (data not shown), which appeared in agreement with previous observations in Heidelberg and Glasgow colonies [5,6]. A semi-quantitative assay by reverse-transcription PCR resulted in no significant differences in brain ANP expression between SHRSP/Izm and SHRSR/Izm. In two independent experiments, densitometric units for SHRSP were 91 and 112% of those for SHRSR, respectively, after normalization by GAPDH levels. An example of the reverse-transcription PCR assay is shown in Fig. 4.

4. Discussion

In the present study, we evaluated the ANP gene in relation to stroke susceptibility through a combination of genetic approaches. Our data failed to support the candidacy at large, but brought up several important issues that require careful interpretation. The issues include: (1) how much statistical value can be set on our association analysis in the Japanese subjects; (2) whether the type of rat ANP alleles accounts for part of phenotypic differences between SHRSP and SHRSR (or WKY) at all; and (3) what are the plausible explanations for the observed discrepancies between two previous studies concerning the rat ANP gene [5,6].

Extending findings in rats to humans is certainly tempting, but results should be critically evaluated as far as the rat data remain undefined. While there was no standard method to etiologically stratify stroke patients according to clinical manifestations, we chose to enroll patients with radiographical evidence of cerebral infarction (i.e. abnormal areas on brain CT or MRI) in order to decrease a genetic diversity in overall stroke. Diagnostic criteria for case subjects were no less stringent than those in the original report [8], where cases were sampled in a population-based setting according to individual's medical records or autopsy results. Since our study was performed in a hospital-based setting, one may argue that the results of association could be affected by insufficient matching of controls or other uncontrolled factors. Several findings can refute this criticism. First, despite the use of different enrollment scheme, comparable results were provided for lack of disease association with the ANP locus in two independent populations. Second, the 664A allele frequencies

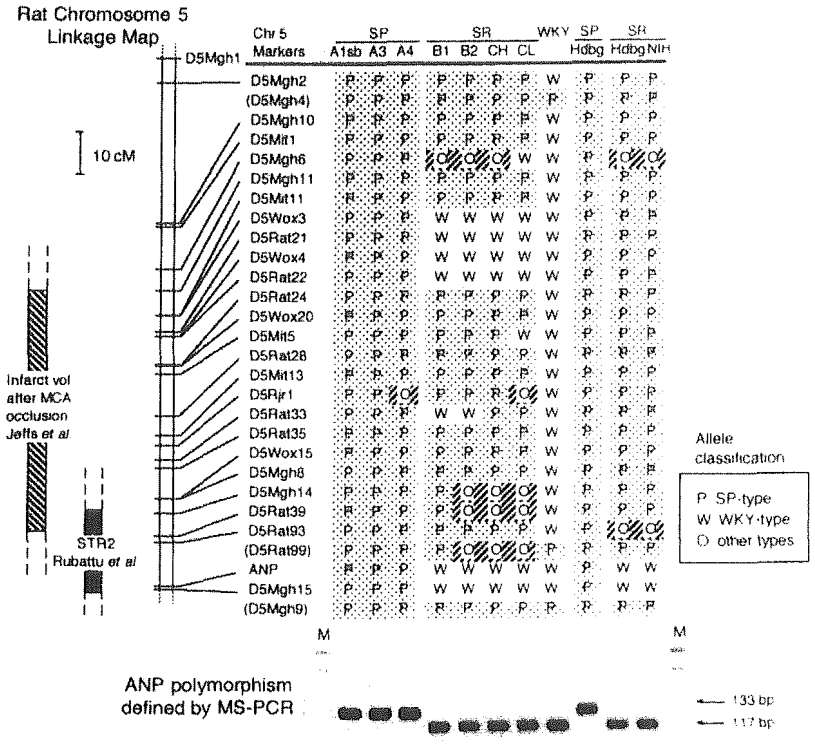

Fig. 3. Substrain comparison in the selected region on rat chromosome 5 (top) and results for an ANP polymorphism defined by MS-PCR (bottom). Marker alleles were categorized into three groups: SP/Izm-type allele (P), WKY/Izm-type allele (W) and alleles different from both types (O). Results for 28 selected markers are depicted in the figure: they were 25 markers informative between A_3 and WKY/Izm and three other markers shown in parentheses. For reference, positions of QTLs for 'stroke-associated' phenotypes are arbitrarily placed to the left of the linkage map, where a likely interval of the QTL for infarct volume after MCA occlusion cannot be precisely defined because Jeffs et al. [6] assigned the ANP locus to the middle of chromosome 5. M, ϕX174 DNA/*Hae*III marker.

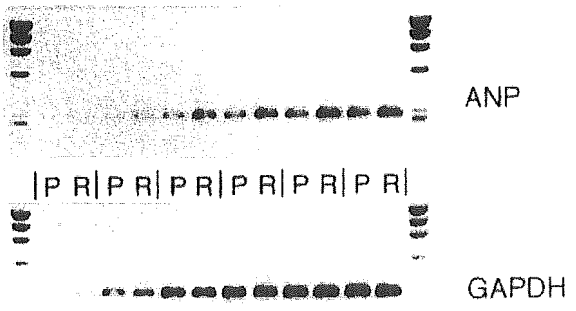

Fig. 4. A quantitative assay by reverse transcription-PCR of brain ANP expression. PCR products were shown with incremental cycles (three additional cycles) from left to right by two consecutive lanes, where products of SHRSP/Izm and SHRSR/Izm were placed in the left and right lanes, respectively. P, SHRSP/Izm; R, SHRSR/Izm.

observed in the present study proved to be concordant with the population frequency (8.9–9.2%) that we previously reported in the Japanese [12]. Furthermore, according to our calculation, a relative risk of > 1.9 could have been detected in the available sample of 270 cases and 359 controls in the first panel alone with 80% power at a 5% type I error probability. This allowed us to test the odds ratio of 2.0, which was shown to be indicative of the risk increase in a white population [8]. Also, it has to be noted that the three tested SNPs could represent principal ANP polymorphisms in the Japanese, as demonstrated by our extensive screening [12].

Then we looked into the candidacy of ANP for rat stroke by comparing substrains of SHR. This strategy is based upon the hypothesis that a gene predisposing rats to stroke should have some functional differences between stroke-prone and stroke-resistant strains. Our results showed that two types of ANP alleles differentiated SHRSP from SHRSR substrains at a structural level. To our surprise, however, WKY/Glasgow appeared to possess a SP/Izm-type allele and, more importantly, apart from four substrains tested in the present study, there was a substrain of SHRSR with a SP/Izm-type allele, which had been extinct and only DNA was available from the frozen liver tissue kept at our institution (data not shown). The presence of 21 polymorphisms between two ANP alleles and the presence of a marker (D15Mgh15) showing the same allele distribution pattern as ANP implied that a certain chromosomal fragment rather than a single de novo mutation of the gene had been inherited during the inbreeding process. Taken together, the following situation is probable. There had been at least two distinct types of ANP alleles among ancestral laboratory rats in Kyoto, Japan, from which SHR and WKY were

developed. A few substrains of SHRSR and WKY should have inherited a SP/Izm-type allele, whereas four SHRSR substrains currently kept in our institution happen to have inherited a WKY/Izm-type allele of ANP.

Before we discuss a functional significance of a SP/Izm-type allele, it seems helpful to review 'stroke-associated' phenotypes in the literature. As for latency until the manifestation of stroke, SHRSP/Heidelberg is assumed to have a 'protective' allele of a QTL postulated on rat chromosome 5 compared with SHRSR/Heidelberg [5,21]. In theory, relating a 'protective' allele to SHRSP ironically counterbalances the propensity for stroke. Because such a QTL is unlikely to constitute a principal determinant for selective breeding of stroke-proneness, a 'protective' allele might as well be found in some substrains of SHRSR and WKY. As for infarct volume after the MCA occlusion (or ischemic vulnerability), on the other hand, significant linkage was identified in F2 progeny between SHRSP/Glasgow and WKY/Glasgow [6]. Even so, it remains unclear whether this trait by itself represents a phenotypic difference between stroke-prone and stroke-resistant SHR strains. Some studies have already shown that ischemic vulnerability is observable in SHRSR and may not account for substantial part of strain differences [22,23]. Thus, considerable care should be exercised when we extend the results for 'stroke-associated' phenotypes to stroke-proneness in SHRSP. Nevertheless, it must be stressed that these arguments do not undermine the original findings of linkage to the individual phenotypes because the existence of QTLs is not questionable under given circumstances, i.e. study design and statistical significance levels presented.

Results of the gene expression study fueled further confusion. We found no significant differences in the brain expression of ANP between SHRSP/Izm and SHRSR/Izm, whereas Rubattu et al. reported 3-fold lower expression in the brain of SHRSP/Heidelberg compared with SHRSR/Heidelberg [7]. This discrepancy may be partly attributed to technical problems, as different quantification methods were used to measure relatively low levels of ANP expression. We should also pay attention to differences in blood pressure (BP) profile between Japanese and Heidelberg colonies: SHRSP promotes a severer degree of hypertension from earlier age of life than SHRSR in an original colony [4], whereas both SHRSP and SHRSR are reported to develop a similar degree of hypertension in a Heidelberg colony [5]. It is therefore possible that BP differences in a Japanese colony (a maximal BP difference exceeds 30–40 mmHg) modify the brain ANP expression towards the reduction of strain differences shown in a Heidelberg colony [7]. In fact, elevated BP was supposed to induce higher mRNA expression of brain ANP in SHR when compared to WKY [24]. Alternatively, despite compelling evidence in experiments in vitro [7], functional alterations of a SP/Izm-type allele may not manifest themselves in vivo dependent on the genetic background, i.e. in SHRSP of a Japanese colony. Further investigations are currently in progress to resolve the uncertainties using a more sensitive quantification technique.

Although human and rat parts of our study do not appear complementary to each other, our data collectively lead to the argument that the ANP gene is unlikely to play a major role in the propensity for stroke. In view of a presumably complex interplay between causative genes and confounding phenotypes, such as hypertension, integration of various genetic strategies is required to clarify the pathophysiological role of the ANP gene in stroke. Findings in the current study are indispensable in this regard.

Acknowledgements

This study was supported by Grants-in-Aid from the Ministry of Education and Science, Japan and a Research Grant of Uehara Memorial Foundation.

References

[1] Graffagnino C, Gasecki AP, Doig GS, Hachinski VC. The importance of family history in cerebrovascular disease. Stroke 1994;25:1599–604.
[2] Okamoto K, Yamori Y, Nagaoka A. Establishment of the stroke-prone spontaneously hypertensive rat (SHR). Circ Res 1974;34–35(Suppl I):143–53.
[3] Yamori Y, Nara Y, Nabika T, Ikeda K, Matsumoto K. Prediction of hypertension and stroke for controlling cardiovascular diseases in genetic rat models. In: Berg K, Bulyzhenkov V, Christen Y, Corvol P, editors. Genetic approaches to coronary heart disease and hypertension. Berlin, Heidelberg: Springer-Verlag, 1991:81–97.
[4] Yamori Y. Development of the spontaneously hypertensive rat (SHR), the stroke-prone SHR (SHRSP) and their various substrain models for hypertension-related cardiovascular diseases. In: Ganten D, de Jong W, editors. Handbook of hypertension, experimental and genetic models of hypertension, vol. 16. Amsterdam: Elsevier Science, 1994:346–64.
[5] Rubattu S, Volpe M, Kreutz R, Ganten U, Ganten D, Lindpaintner K. Chromosomal mapping of quantitative trait loci contributing to stroke in a rat model of complex human disease. Nat Genet 1996;13:429–34.
[6] Jeffs B, Clark JS, Anderson NH, Gratton J, Brosnan J, Gauguier D, et al. Sensitivity to cerebral ischemic insult in a rat model of stroke is determined by a single genetic locus. Nat Genet 1997;16:364–7.
[7] Rubattu S, Kirsch AL, DePaolis P, Giliberti R, Gigante B, Lombardi A, et al. Altered structure, regulation, and function of the gene encoding the atrial natriuretic peptide in the stroke-prone spontaneously hypertensive rat. Circ Res 1999;85:900–5.
[8] Rubattu S, Ridker P, Stampfer MJ, Volpe M, Hennekens CH, Lindpaintner K. The gene encoding atrial natriuretic peptide and the risk of human stroke. Circulation 1999;100:1722–6.

[9] Brosnan MJ, Clark JS, Jeffs B, Negrin CD, Van Vooren P, Arribas SM, et al. Genes encoding atrial and brain natriuretic peptides as candidates for sensitivity to brain ischemia in stroke-prone hypertensive rats. Hypertension 1999;33(Part 2):290–7.
[10] Kato N, Morita H, Sugiyama T, Kurihara H, Tsubaki S, Nabika T, et al. Evaluation of the poly(ADP-ribose) polymerase gene in human stroke. Atherosclerosis 2000;148:345–52.
[11] Notsu Y, Nabika T, Park HY, Masuda J, Kobayashi S. Evaluation of genetic risk factors for silent brain infarction. Stroke 1999;30:1881–6.
[12] Kato N, Sugiyama T, Morita H, Nabika T, Kurihara H, Yamori Y, et al. Genetic analysis of the atrial natriuretic peptide gene in essential hypertension. Clin Sci 2000;98:251–8.
[13] Okamoto K, Hazama F, Yamori Y, Haebara H, Nagaoka A. Pathogenesis and prevention of stroke in spontaneously hypertensive rats. Clin Sci Mol Med 1975;48:161s–3s.
[14] Stolley PD, Schlesselman JJ. Multivariate analysis. In: Schlesselman JJ, editor. Case-control studies. Oxford: Oxford University Press, 1982:227–90.
[15] Okamoto K, Yamori Y, Ooshima A, Park C, Haebara H, Matsumoto M, et al. Development and heredity: establishment of the inbred strain of the spontaneously hypertensive rat and genetic factors involved in hypertension. In: Okamoto K, editor. Spontaneous hypertension. Tokyo: Springer–Igaku Shoin, 1972:1–8.
[16] Nabika T, Nara Y, Ikeda K, Endo J, Yamori Y. Genetic heterogeneity of the spontaneously hypertensive rat. Hypertension 1991;18:12–6.
[17] Kato N, Tamada T, Nabika T, Ueno K, Gotoda T, Matsumoto C, et al. Identification of quantitative trait loci for serum cholesterol levels in stroke-prone spontaneously hypertensive rats. Arterioscler Thromb Vasc Biol 2000;20:223–9.
[18] Rust S, Funke H, Assmann G. Mutagenically separated PCR (MS-PCR): a high specific one step procedure for easy mutation detection. Nucleic Acids Res 1993;21:3623–9.
[19] Rosenzweig A, Halazonetis TD, Seidman JG, Seidman CE. Proximal regulatory domains of rat atrial natriuretic factor gene. Circulation 1991;84:1256–65.
[20] Kozak M. An analysis of 5′-noncoding sequences from 699 vertebrate messenger RNAs. Nucleic Acids Res 1987;15:8125–48.
[21] Rubattu S, Giliberti R, Ganten U, Volpe M. Differential brain atrial natriuretic peptide expression co-segregates with occurrence of early stroke in the stroke-prone phenotype of the spontaneously hypertensive rat. J Hypertens 1999;17:1849–52.
[22] Coyle P. Different susceptibilities to cerebral infarction in spontaneously hypertensive (SHR) and normotensive Sprague–Dawley rats. Stroke 1986;17:520–5.
[23] Duverger D, MacKenzie ET. The quantification of cerebral infarction following focal ischemia in the rat: influence of strain, arterial pressure, blood glucose concentration, and age. J Cereb Blood Flow Metab 1988;8:449–61.
[24] Komatsu K, Tanaka I, Funai T, Ichiyama A, Yoshimi T. Increased level of atrial natriuretic peptide messenger RNA in the hypothalamus and brainstem of spontaneously hypertensive rats. J Hypertens 1992;10:17–23.

Role of Endogenous Adrenomedullin in the Regulation of Vascular Tone and Ischemic Renal Injury

Studies on Transgenic/Knockout Mice of Adrenomedullin Gene

Hiroaki Nishimatsu, Yasunobu Hirata, Takayuki Shindo, Hiroki Kurihara, Masao Kakoki, Daisuke Nagata, Hiroshi Hayakawa, Hiroshi Satonaka, Masataka Sata, Akihiro Tojo, Etsu Suzuki, Kenji Kangawa, Hisayuki Matsuo, Tadaichi Kitamura, Ryozo Nagai

Abstract—Adrenomedullin (AM) is a potent depressor peptide whose vascular action is suggested to involve nitric oxide (NO) release. To explore the role of endogenous AM in vascular and renal function, we examined the effects of acetylcholine (ACh), AM, and AM receptor antagonists AM(22-52) and CGRP(8-37) on the renal perfusion pressure (RPP) of kidneys isolated from AM transgenic (TG)/heterozygote knockout (KO) mice and wild-type littermates (WT). Furthermore, we evaluated the renal function and histology 24 hours after bilateral renal artery clamp for 45 minutes in TG, KO, and WT mice. Baseline RPP was significantly lower in TG than in KO and WT mice (KO 93.4±4.6, WT 85.8±4.2, TG 72.4±2.4 mm Hg [mean±SE], $P<0.01$). ACh and AM caused a dose-related reduction in RPP, but the degree of vasodilatation was smaller in TG than that in KO and WT (%ΔRPP 10^{-7} mol/L ACh: KO −48.1±3.9%, WT −57.5±5.6%, TG −22.8±4.8%, $P<0.01$), whereas N^G-nitro-L-arginine methyl ester (L-NAME) caused greater vasoconstriction in TG (%ΔRPP 10^{-4} mol/L: KO 33.1±3.3%, WT 55.5±7.2%, TG 152.6±21.2%, $P<0.01$). Both AM antagonists increased RPP in TG to a greater extent compared with KO and WT mice (%ΔRPP 10^{-6} mol/L CGRP(8-37): KO 12.8±2.6%, WT 19.4±3.6%, TG 41.8±8.7%, $P<0.01$). In mice with ischemic kidneys, serum levels of urea nitrogen and renal damage scores showed smaller values in TG and greater values in KO mice (urea nitrogen: KO 104±5>WT 98±15>TG 38±7 mg/dL, $P<0.05$ each). Renal NO synthase activity was also greater in TG mice. However, the differences in serum urea nitrogen and renal damage scores among the 3 groups of mice were not observed in mice pretreated with L-NAME. In conclusion, AM antagonists increased renal vascular tone in WT as well as in TG, suggesting that endogenous AM plays a role in the physiological regulation of the vascular tone. AM is likely to protect renal tissues from ischemia/reperfusion injury through its NO releasing activity. ***(Circ Res. 2002;90:657-663.)***

Key Words: adrenomedullin ■ nitric oxide ■ cGMP ■ endothelium ■ ischemia

Adrenomedullin (AM) is a potent vasodilating peptide that was originally isolated from human pheochromocytoma cells.[1] AM has been considered a member of the calcitonin gene-related peptide (CGRP) superfamily based on their structural similarities. In fact, both peptides are reported to share common receptors. At present, it is known that AM-producing cells widely distribute in the whole body including the adrenal glands, heart, lungs, and kidneys. However, there is no step-up in AM levels of the venous plasma drained from various organs.[2] It has also been reported that cultured vascular smooth muscle cells and endothelial cells synthesize and secrete AM.[3,4] These findings suggest that circulating AM derives mainly from vascular walls and plays a role in the vascular system.

Because AM is isolated on the basis of the cAMP-increasing activity,[1] at first cAMP was considered to be the sole second messenger for AM-induced vasodilation.[5,6] However, it was reported that AM dilates vessels in an endothelium-dependent manner and that cGMP is another second messenger for AM.[7–11] We have already reported that denudation of rat aortic endothelial cells and inhibition of guanylate cyclase substantially inhibited AM-induced vasodilation.[11] Furthermore, AM increased nitric oxide (NO) release from rat perfused kidneys and inhibition of NO synthase decreased both NO release and vasodilation caused by AM.[8] These findings suggest that AM-induced vasodilation is partly dependent of activation of the NO-cGMP pathway.

Plasma levels of AM are elevated in patients with hypertension, heart failure, or renal failure.[2,12,13] Because AM exerts vasodilatory and natriuretic effects, the increased levels of AM have been considered to play a compensatory role under such pathological conditions. However, plasma

Original received August 24, 2001; revision received January 3, 2002; accepted February 11, 2002.

From the Departments of Urology (H.N., T.K.) and Internal Medicine (Y.H., T.S., H.K., M.K., D.N., H.H., H.S., M.S., A.T., E.S., R.N.), Faculty of Medicine, The University of Tokyo; and the Research Institute (K.K., H.M.), National Center of Cardiovascular Medicine, Japan.

Correspondence to Yasunobu Hirata, MD, Dept of Cardiovascular Medicine, The University of Tokyo, 7-3-1 Hongo, Bunkyo-ku, Tokyo 113-8655, Japan. E-mail hirata-2im@h.u-tokyo.ac.jp

Circulation Research is available at http://www.circresaha.org DOI: 10.1161/01.RES.0000013697.55301.E7

levels of AM in the healthy populations are low and they show only several-fold increases even in patients with heart failure.[2,12,13] Thus, it is unclear as to whether endogenous AM plays a significant role under physiological conditions. Recent progress of genetic technologies has enabled us to determine the in vivo activities of endogenous bioactive substances. We have recently established some mice strains in which AM genes are overexpressed or disrupted. Mice showing overexpression of AM genes, that is AM transgenic (TG) mice, had hypotension,[14] whereas disruption of the AM gene was lethal. Heterozygote mice with a disrupted AM gene ($AM^{+/-}$ mice; KO) showed slight increases in blood pressure, compared with wild-type (WT) mice.[15]

Although NO has various cardiovascular effects, its role in ischemia/reperfusion renal injury is still controversial.[16–19] We have reported that in ischemic acute renal failure (iARF) increases in endothelium-derived NO mitigated renal injury and vice versa.[19] If AM releases substantial amounts of NO from the renal vasculature, increases in endogenous AM may be beneficial for ischemic renal injury. Thus, we analyzed the role of endogenous AM in the regulation of aortic and renal vascular tone and in renal injury caused by ischemia/reperfusion using AM TG mice and KO mice.

Materials and Methods

Animals

All mouse studies were performed in concordance with the university guidelines for animal experiments. AM TG mice and KO mice were established as previously reported. TG mice were established using fusion cDNA of the AM gene with the preproendothelin-1 gene, resulting in overexpression of AM in the vascular wall, particularly in the endothelium, and 2- to 5-fold increases in AM expression in the aorta and kidneys.[14] AM KO mice were established by replacing exon 1 to 4 with the neomycin-resistant gene. Because AM homozygote KO mice were lethal, we used heterozygote mice as AM KO mice in which the AM content in the heart and lung decreased to 50% of that in WT mice.[15]

Radioimmunoassay for Adrenomedullin

Adrenomedullin concentration in the kidney of 12-week old AM TG mice, AM KO mice, and WT mice was measured by radioimmunoassay (RIA) as previously described.[20] Under anesthesia induced with 40 mg/kg pentobarbital IP, the right kidney was isolated and homogenized (n=5). The homogenate was concentrated using Sep-Pak C18 cartridges and then dissolved in 100 μL of RIA buffer.

Isolated Perfused Kidney

Male AM TG (n=7), KO (n=6), and WT (n=6) mice were anesthetized with 40 mg/kg pentobarbital IP, then the right kidney was isolated and perfused as previously described.[21,22] In brief, after an abdominal incision, we punctured the superior mesenteric artery with a needle and positioned the tip in the right renal artery. Perfusion was then started at 1.5 mL/min with Krebs-Henseleit buffer, and the kidney was isolated without ischemia. The buffer was saturated with 95% O_2/5% CO_2 at 37°C and contained 10^{-6} mol/L angiotensin II and 10^{-5} mol/L indomethacin to maintain perfusion pressure at about 100 mm Hg. Renal perfusion pressure (RPP) was monitored at the renal artery through the needle connected to a pressure transducer (Datex-Ohmeda K.K., Tokyo).

Measurement of NO Release

NO concentration in the perfusate was measured using a chemiluminescence assay.[22] The venous effluent was introduced into a rotatory mixer with a chemiluminescence probe of 10 mmol/L H_2O_2, 18 μmol/L recrystallized luminol, 2 mmol/L potassium carbonate, and 150 mmol/L desferrioxamine. The mixture of the perfusate and probe then entered a chemiluminescence detector. The chemiluminescent signal was measured continuously and recorded on a standard pen recorder. The NO signal was calibrated using an NO solution.

Following a 60-minute equilibrium period, graded doses of ACh or AM were added to the buffer at 10-minute intervals through a 3-way cock. The responses to N^G-nitro-L-arginine methyl ester (L-NAME), an NO synthase (NOS) inhibitor, AM(22-52) and CGRP(8-37), AM receptor antagonists, or E-4021 (Eisai Co, Ltd), a phosphodiesterase (PDE) inhibitor, were studied in the same manner. E-4021 is a type-V PDE inhibitor that has been reported to selectively inhibit cGMP-specific PDE.[23] To evaluate the effects of NOS or PDE inhibition, the effects of N^G-monomethyl-L-arginine (L-NMMA) or E-4021 infusion on RPP were examined. NO release was normalized by kidney weight and expressed as fmol per minute per gram kidney weight.

Ischemic Acute Renal Failure

Twelve-week-old AM TG (n=10), KO (n=10), and WT (n=10) male mice were used in the present study. The in vivo model of iARF was prepared as described elsewhere.[19] In brief, after anesthesia with pentobarbital sodium (40 mg/kg IP), a midline abdominal incision was made and bilateral renal arteries were clamped with plastic clips for 45 minutes after the injection of heparin (10 U/kg, IM); thereafter, the clamps were removed and the incision was closed. Twenty-four hours after the start of reperfusion, 0.3 mL arterial blood was drawn to determine the serum levels of urea nitrogen and creatinine. Thereafter, the kidneys were perfused with saline for histological studies. The NOS inhibitor, L-NAME (30 mg/kg), was administered by gavage to 5 of each mice group before induction of renal ischemia.

Histological Studies

Samples of renal tissue from the sham-operated and ischemic animals were fixed in 10% formaldehyde, stained with periodic acid-Schiff's (PAS) reagent, and examined under an optical microscope in a blinded manner. The kidneys were histologically examined for the presence of dilatation of Bowman's space, tubular dilatation and necrosis, loss of tubular epithelium, and tubular casts. The degree of renal injury was evaluated using the criteria reported by Solez et al.[24]

Measurement of NOS Activity

The activity of NOS in vitro was determined by the conversion of L-[^{14}C] arginine to L-[^{14}C] citrulline, according to the method described previously.[19] The renal medulla was dissected and homogenized in lysis buffer. Forty μL of the sample was incubated in 100 μL of assay buffer containing 0.5 mCi/mL L-[^{14}C] arginine and incubated for 20 minutes at 37°C. To separate L-[^{14}C] arginine from L-[^{14}C] citrulline, the samples were loaded onto 1-mL columns of Dowex resin (AG50WX-8 Na^+ form) and eluted with 500 μL distilled water. Aliquots were used for liquid scintillation counting. Calcium-dependent activity was determined as the difference between the L-[^{14}C] citrulline produced from control samples and samples containing 3 mmol/L EGTA to bind calcium.

Drugs and Chemicals

Laboratory reagents and chemicals used to prepare Krebs-Henseleit solution and H_2O_2 were purchased from Wako Pure Chemicals (Osaka). AM, AM(22-52), and CGRP(8-37) were from the Peptide Institute (Osaka). All other chemicals were from Sigma-Aldrich Japan (Tokyo).

Statistical Analysis

Data are expressed as the mean±SEM. Statistical comparisons were made by analysis of variance followed by the Student-Neumann-Keuls test. To compare renal injury scores, the nonparametric

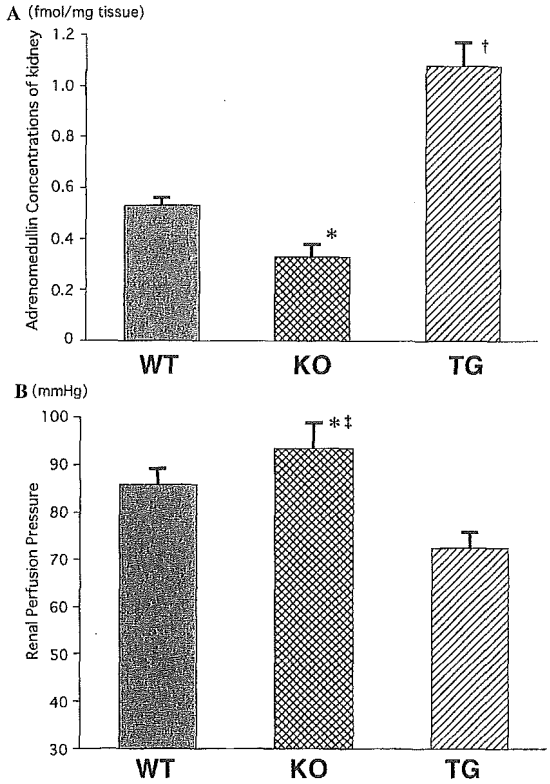

Figure 1. Adrenomedullin (AM) concentrations of the kidneys (A) and baseline renal perfusion pressure (B) isolated from AM transgenic (TG) mice, AM knockout (KO) mice, and wild-type (WT) mice. *$P<0.01$, †$P<0.001$ vs WT; ‡$P<0.001$ vs TG.

Kruskal-Wallis test was used. Differences with a value of $P<0.05$ were considered statistically significant.

Results

Renal Contents of AM

We measured the renal contents of AM in the 3 groups of mice by RIA. As shown in Figure 1A, AM contents in the kidney of AM TG mice were significantly greater than WT mice, whereas those of AM KO mice were significantly less. These results were compatible with the findings of our previous reports.[14,15]

Isolated Perfused Kidney

Kidneys from KO, TG, and WT mice were macroscopically normal and their weight did not greatly differ among the 3 groups. Baseline RPP in KO mice was significantly higher, whereas that in TG mice was lower, compared with RPP in WT mice kidneys (Figure 1B).

Figure 2 shows the effects of ACh on RPP and NO release in the 3 groups of mice kidneys. ACh lowered RPP of kidneys in either group in a dose-related manner. The degree of renal vasodilation caused by ACh was smaller in TG mice than in WT and KO mice. The ACh-induced vasodilation was associated with an increase in NO release from the kidney. NO release caused by ACh was greater in TG mice and smaller in KO mice, compared with WT mice. Thus, TG mice kidneys showed hyporesponsiveness to NO. The responses to AM in the 3 groups of mice were similar to those to ACh (data not shown). Figures 3A and 3B shows the effects of AM receptor antagonists AM(22-52) and CGRP(8-37) on RPP, respectively. Both antagonists alone significantly elevated RPP in a dose-related fashion. The increase in RPP was significant even in KO and WT mice. The response decreased in the following order: TG>WT>KO.

In order to explore the involvement of the NO-cGMP pathway in AM-induced vasodilation, we examined the effects of L-NMMA and E-4021 on RPP. As shown in Figure 3C, L-NMMA alone increased RPP in all 3 groups of kidneys. In contrast, E-4021 alone reduced RPP (Figure 3D). These changes in RPP caused by L-NMMA and E-4021 were dose-related and the responses decreased in the following order: TG>WT>KO.

Ischemic Acute Renal Failure

No mice died after renal ischemia/reperfusion. Serum concentrations of urea nitrogen markedly increased 24 hours after reperfusion in WT mice (Figure 4A). Decreases in renal excretory function were significantly greater in KO mice than in WT mice. However, the increases in urea nitrogen levels were significantly smaller in TG mice. Serum creatinine levels changed almost in parallel with urea nitrogen levels in the 3 groups of mice (Figure 4B). Pretreatment with L-NAME did not change the increases in serum urea nitrogen levels in WT and KO mice, whereas it significantly increased them in TG mice, resulting in no differences in serum urea nitrogen or creatinine levels among the 3 groups of mice.

Changes in renal excretory function induced by ischemia were confirmed by histological analysis. Figure 5 shows the renal histology of the 3 groups of mice. In WT mice, marked damage of renal tissues, particularly in the tubuli, were observed; these included detachment of epithelial cells of the proximal tubuli, interstitial edema, and tubular casts. Expansion of Bowman's space was also observed. AM KO mice also had marked tubular damage. However, in AM TG mice

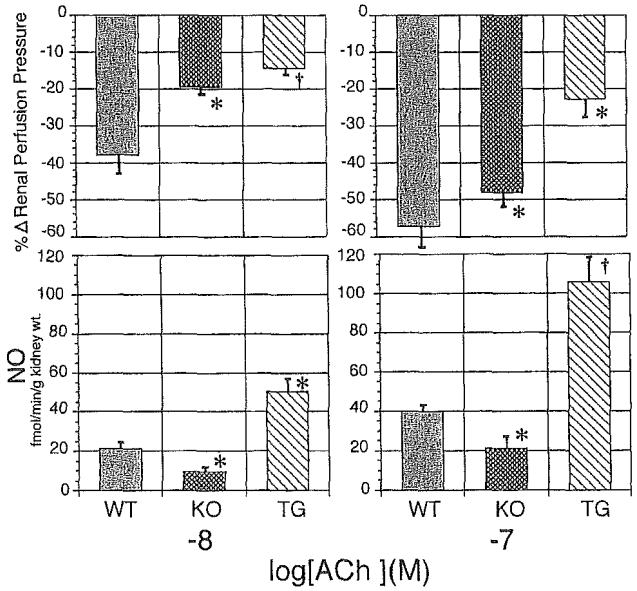

Figure 2. Effects of acetylcholine (ACh) on renal perfusion pressure (RPP) and release of NO in TG, WT, and KO mice. *$P<0.05$, †$P<0.01$ vs WT.

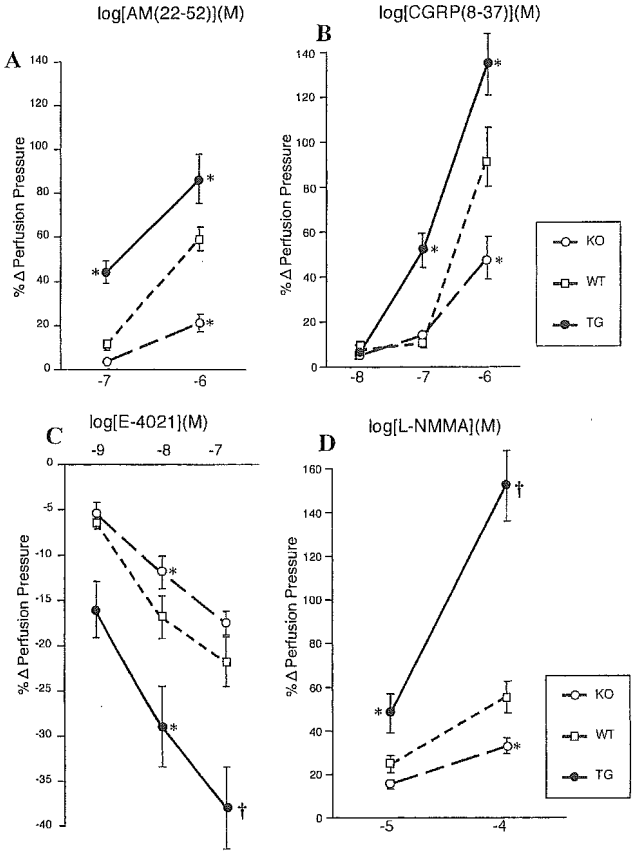

Figure 3. Effects of adrenomedullin (AM) receptor antagonists, AM(22-52) (A) and CGRP(8-37) (B), on renal perfusion pressure (RPP) in TG, WT, and KO mice. Effects of E-4021 (C) and N^G-monomethyl-L-arginine (L-NMMA) (D) on renal perfusion pressure (RPP) in TG, WT, and KO mice. *$P<0.05$, †$P<0.01$ vs WT.

renal injury was apparently mild. In fact, all 4 types of damage scores were significantly less marked in TG mice compared with the other 2 groups of mice. Figure 6 shows the means of 4 types of injury scores in each group of mice. AM KO mice kidneys subjected to ischemia showed significantly greater scores than WT mice and AM TG mice. Pretreatments with L-NAME also diminished differences in renal injury scores among the 3 groups of mice.

Renal NOS Activity

As shown in Figure 7, calcium-dependent NOS activity in the renal medulla was greater in TG mice, whereas it tended to be less in KO mice. Ischemia/reperfusion decreased the NOS activity in all 3 groups of mice. However, the NOS activity was still greater in TG mice kidneys. On the other hand, calcium-independent NOS activity was not detected in the kidney of any group of animals.

Discussion

Endothelial cells secrete many circulating and local vasoactive hormones. Among them, endothelin-1 and NO are potent vasoconstrictive and vasodilative substances, respectively, and they play important roles because their gene disruption results in death or in a hypertensive reaction, respectively.[25,26] However, it has not been clarified whether endothelium-derived AM is a significant factor in the regulation of circulation.

The plasma concentration of AM in healthy subjects is at a picomolar level.[1,7] However, the vasodilatory effects of AM appear at concentrations higher than 10^{-10} mol/L, according to previous reports.[14] In the present study, significant vasodilation in the renal vessels and aorta was observed also at about 10^{-9} mol/L. That is, the physiological circulating level of AM is about a hundredth of the effective concentration on arteries, although it is possible that the vascular wall may be exposed to locally high concentrations of AM. Receptor antagonists are useful tools to explore the role of endogenous ligands. We examined 2 kinds of AM receptor antagonists, CGRP(8-37)[27] and AM(22-52).[5] Both antagonists increased the vascular tone in renal vessels precontracted by angiotensin II in a dose-related manner. This suggests that endogenous AM in the vasculature shows tonic inhibition on vasoconstrictive stimuli. This phenomenon may be explained by some agonistic action of the antagonists, particularly at higher concentrations. In fact, AM(1-25), a truncated peptide of AM, exerts vasoconstrictive activity.[28] However, CGRP derivatives have not been reported to cause vasoconstriction.

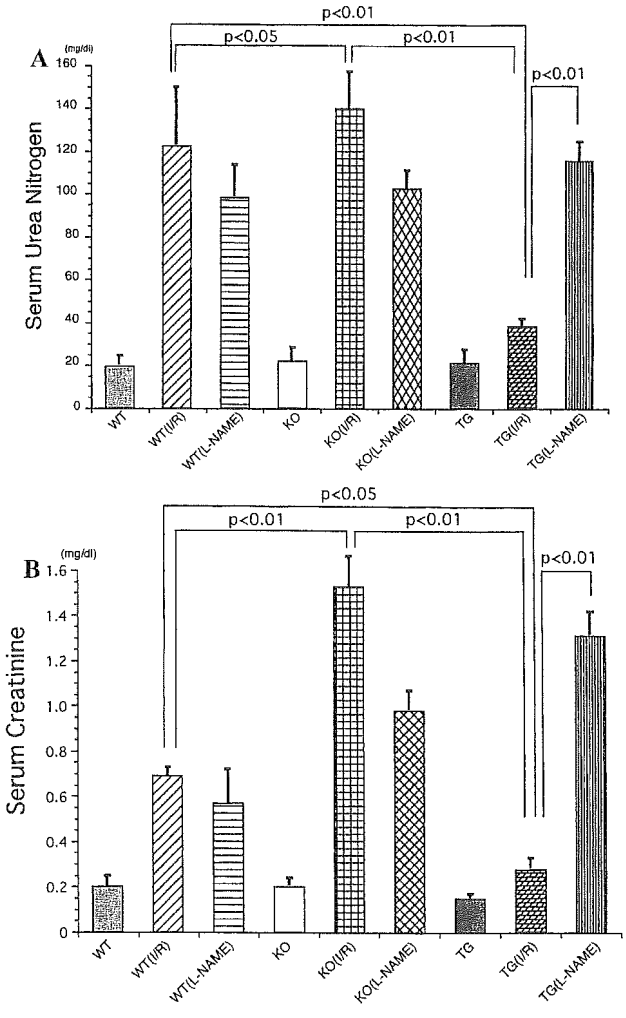

Figure 4. Serum urea nitrogen (A) and creatinine levels (B) in mice with ischemic acute renal failure. (I/R) indicates ischemia/reperfusion; L-NAME, N^G-nitro-L-arginine methyl ester+I/R.

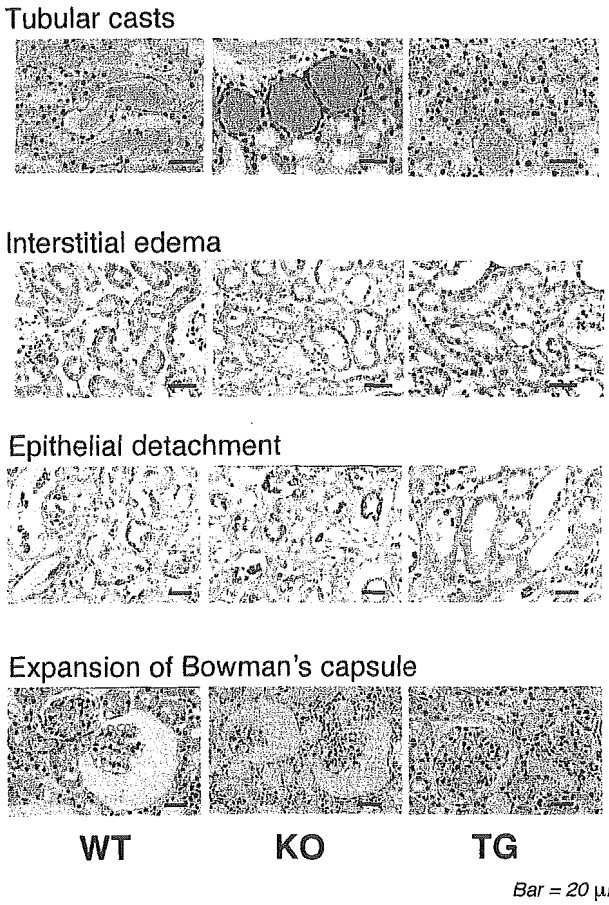

Figure 5. Photographs of renal histology showing tubular casts, interstitial edema, epithelial detachment, and expansion of Bowman's capsule from AM transgenic (TG) mice, AM knockout (KO) mice, and wild-type (WT) mice.

Furthermore, because endothelial denudation of the aorta diminished the vasoconstriction caused by receptor antagonists (unpublished observation, 2001), it is unlikely that the two antagonists per se increased vascular tone. Thus, it appears that the antagonists-induced vasoconstriction is attributed to a direct blockade of the action of endogenous AM.

It is striking that the receptor antagonists significantly increased RPP even in WT mice, although vasoconstriction was greater in TG mice and less in KO mice. Baseline perfusion pressure in the kidney isolated from KO mice was significantly higher than that from WT mice. These findings suggest that endogenous AM actually regulates renal vascular tone under physiological conditions, at least in mice. Furthermore, the decrease in endogenous AM production by 50% may contribute to increases in renal vascular resistance. It is not exceptional that a 50% reduction of gene expression influences its function. For example, heterozygote eNOS KO mice showed slightly higher blood pressure[29] and greater susceptibility to pulmonary hypertension due to hypoxia than WT mice.[30] Although it is unknown whether there is a pathological state associated with a reduced production of AM, various cardiovascular diseases are associated with several-fold increases in circulating AM.[2,12,13] In TG mice, expression of AM in the aorta and kidney increased by 2- to 5-fold.[14] Therefore, increased AM in patients with hypertension and chronic renal failure may play a compensatory role with regard to blood pressure regulation. On the other hand, in septic shock in which the highest level of plasma AM was reported,[31,32] AM may be one of the factors contributing to hypotension. In the present study, compared with WT mice, TG mice showed 2-fold increase and KO mice about 50% decrease in AM. Thus, the AM levels in TG and KO mice were pathological rather than physiological. In iARF, AM KO mice subjected to ischemia/reperfusion had significantly higher serum urea nitrogen and creatinine levels than WT mice. Furthermore, histological analysis revealed that renal damage was significantly more severe in KO mice than in WT mice. These results suggest that high levels of AM may mitigate renal damage and decreases of AM below the physiological level may abrogate it.

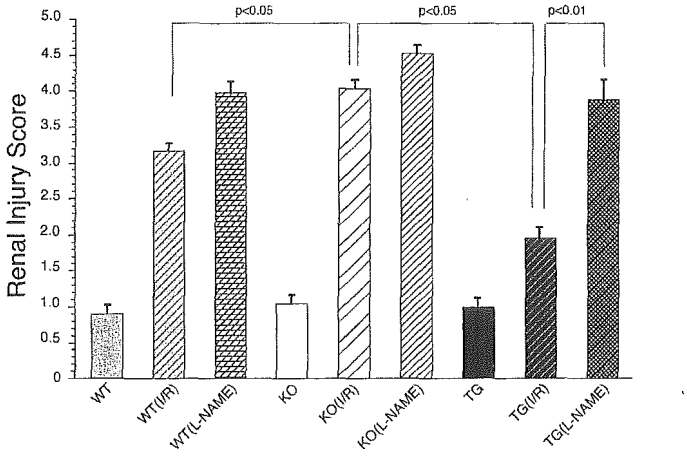

Figure 6. Effects of ischemia and preischemic treatment with L-NAME on renal injury scores in TG, WT, and KO mice. Values are means of 4 types of injury scores. (I/R) indicates ischemia/reperfusion; L-NAME, L-NAME+I/R.

Not only AM-induced vasodilation but also ACh-induced vasodilation was attenuated in AM TG mice. This mechanism is unclear from the present study; however, eNOS TG mice

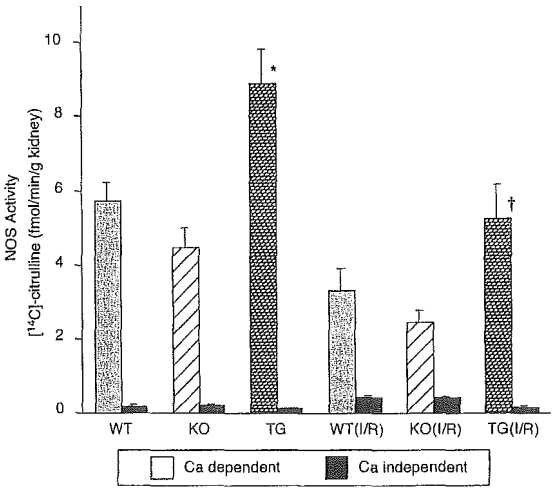

Figure 7. NO synthase activity in the kidneys of TG, WT, and KO mice. NO synthase activity was measured based on the conversion of L-arginine to L-citrulline. (I/R) indicates ischemia/reperfusion. *$P<0.05$ vs WT; †$P<0.05$ vs WT(I/R).

also showed hyporesponsiveness to endothelium-dependent vasodilators, but not to endothelium-independent vasodilators.[33] In these mice, the activity of soluble guanylate cyclase and the expression of cGMP-dependent protein kinase decreased, probably due to continuous activation of the NO-cGMP pathway.[34] A similar kind of downregulation of the signal transduction of the NO system may occur in AM TG mice. However, this mechanism may not totally explain the differences in vasodilatory responses of the 3 groups of mice because NO synthase inhibition increased RPP in AM TG mice to a greater extent. The responses to L-NMMA or E-4021 reflected the baseline NO releasing rates. The response of TG mice to NO may be attenuated. However, blood pressure and RPP in TG mice were still significantly lower, suggesting that the total vascular effects of endogenous NO in TG mice may overwhelm the attenuated response and be greater than those in WT mice at the baseline level. Thus, the differences in the responses to L-NMMA and E-4021 suggest the great differences in baseline NO release among the mice groups. On the other hand, when NO release was stimulated, nearly maximal renovasorelaxation in AM TG mice may at least in part explain the mechanism for attenuated vasodilatory responses to ACh. This is compatible with the findings of previous reports that L-NMMA caused greater vasoconstriction under increased NO release, including eNOS transgenic mice.[33,34]

In the present study, 24-hour reperfusion following 45-minute ischemia caused iARF in mice. Although many factors may involve renal injury caused by ischemia/reperfusion, the role of NO has been considered to be important; however, it is still controversial as to whether NO increases or decreases and as to which NO synthase is responsible for the change in NO in iARF. We have recently reported that tetrahydrobiopterin (BH4), a cofactor of NO synthase, of renal tissue is deficient in iARF and that replacement of BH4 restored renal endothelium-derived NO and improved renal injury in rats.[19] On the other hand, inhibition of NO synthesis by L-NAME aggravated renal injury. These findings suggest that endothelium-derived NO exerts cytoprotective effects in ischemia/reperfusion and its decrease enhances tissue injury. From this point of view, in TG mice the degree of renal injury and renal excretory dysfunction was less than in WT mice, suggesting that AM-induced NO release may contribute to mitigation of ischemic renal injury. In fact, renal NOS activity increased in AM TG mice. Pretreatment with L-NAME abolished the differences in renal function between TG mice and WT mice, supporting this possibility. It remains undetermined as to how NO mitigates ischemia/reperfusion injury. However, it is possible that NO is a potent antioxidant and traps superoxide during the reperfusion period. Furthermore, it has been reported that NO suppresses excessive increases in intracellular calcium by increasing cGMP.[35] NO-induced vasodilation also contributes to it. AM is reported to protect cultured endothelial cells from apoptosis and this effect is mediated by the stimulation of NO production by endothelial cells.[36]

From the results of L-NMMA administration and citrulline assay, we supposed that AM-induced renal protection might be exerted via NO release. The citrulline assay showed that the NOS activity was much lower in the renal cortex of all groups of mice than in the medulla. This finding was consistent with that of most previous studies, which found that NOS activity in the renal cortex was less than 10% of that in the medulla.[37–39] Because it is difficult to differentiate a calcium-dependent activity of NOS from a calcium-independent one, we did not analyze the small activity detected in the renal cortex. Although it is possible that NO released in the cortex may also work, it is suggested that NO derived from medullary vessels and tubuli would play a major role in protecting renal function.[40]

In conclusion, using genetically manipulated animals, we found that endogenous AM actually regulates renal vascular tone even by relatively small changes in its production. Furthermore, AM may exert a cytoprotective role in ischemic injury through its NO-releasing activity.

Acknowledgments

This study was supported in part by Grants-in-Aid Nos. 10218202, 13470141, and 13557061 from the Japanese Ministry of Education, Culture, Sports and Science. We thank Marie Morita, Reiko Sato, and Etsuko Taira for technical assistance.

References

1. Kitamura K, Kangawa K, Kawamoto M, Ichiki Y, Nakamura S, Matsuo H, Eto T. Adrenomedullin: a novel hypotensive peptide isolated from human pheochromocytoma. *Biochem Biophys Res Commun.* 1993;192:553–560.
2. Nishikimi T, Saito Y, Kitamura K, Ishimitsu T, Eto T, Kangawa K, Matsuo H, Omae T, Matsuoka H. Increased plasma levels of adrenomedullin in patients with heart failure. *J Am Coll Cardiol.* 1995;26:1424–1431.
3. Sugo S, Minamino N, Shoji H, Kangawa K, Kitamura K, Eto T, Matsuo H. Interleukin-1, tumor necrosis factor and lipopolysaccharide additively stimulate production of adrenomedullin in vascular smooth muscle cells. *Biochem Biophys Res Commun.* 1995;207:25–32.
4. Sugo S, Minamino N, Kangawa K, Miyamoto K, Kitamura K, Sakata J, Eto T, Matsuo H. Endothelial cells actively synthesize and secrete adrenomedullin [published erratum appears in *Biochem Biophys Res Commun* 1994;203:1363]. *Biochem Biophys Res Commun.* 1994;201:1160–1166.
5. Eguchi S, Hirata Y, Iwasaki H, Sato K, Watanabe TX, Inui T, Nakajima K, Sakakibara S, Marumo F. Structure-activity relationship of adrenomedullin, a novel vasodilatory peptide, in cultured rat vascular smooth muscle cells. *Endocrinology.* 1994;135:2454–2458.
6. Ishizaka Y, Tanaka M, Kitamura K, Kangawa K, Minamino N, Matsuo H, Eto T. Adrenomedullin stimulates cyclic AMP formation in rat vascular smooth muscle cells. *Biochem Biophys Res Commun.* 1994;200:642–646.
7. Shimekake Y, Nagata K, Ohta S, Kambayashi Y, Teraoka H, Kitamura K, Eto T, Kangawa K, Matsuo H. Adrenomedullin stimulates two signal transduction pathways, cAMP accumulation and Ca^{2+} mobilization, in bovine aortic endothelial cells. *J Biol Chem.* 1995;270:4412–4417.
8. Hirata Y, Hayakawa H, Suzuki Y, Suzuki E, Ikenouchi H, Kohmoto O, Kimura K, Kitamura K, Eto T, Kangawa K, et al. Mechanisms of adrenomedullin-induced vasodilation in the rat kidney. *Hypertension.* 1995;25:790–795.
9. Miura K, Ebara T, Okumura M, Matsuura T, Kim S, Yukimura T, Iwao H. Attenuation of adrenomedullin-induced renal vasodilatation by N^G-nitro L-arginine but not glibenclamide. *Br J Pharmacol.* 1995;115:917–924.
10. Majid DS, Kadowitz PJ, Coy DH, Navar LG. Renal responses to intra-arterial administration of adrenomedullin in dogs. *Am J Physiol.* 1996;270:F200–F205.
11. Hayakawa H, Hirata Y, Kakoki M, Suzuki Y, Nishimatsu H, Nagata D, Suzuki E, Kikuchi K, Nagano T, Kangawa K, Matsuo H, Sugimoto T, Omata M. Role of nitric oxide-cGMP pathway in adrenomedullin-induced vasodilation in the rat. *Hypertension.* 1999;33:660–665.

12. Ishimitsu T, Nishikimi T, Saito Y, Kitamura K, Eto T, Kangawa K, Matsuo H, Omae T, Matsuoka H. Plasma levels of adrenomedullin, a newly identified hypotensive peptide, in patients with hypertension and renal failure. *J Clin Invest.* 1994;94:2158–2161.
13. Jougasaki M, Wei CM, McKinley LJ, Burnett JC Jr. Elevation of circulating and ventricular adrenomedullin in human congestive heart failure. *Circulation.* 1995;92:286–289.
14. Shindo T, Kurihara H, Maemura K, Kurihara Y, Kuwaki T, Izumida T, Minamino N, Ju KH, Morita H, Oh-hashi Y, Kumada M, Kangawa K, Nagai R, Yazaki Y. Hypotension and resistance to lipopolysaccharide-induced shock in transgenic mice overexpressing adrenomedullin in their vasculature. *Circulation.* 2000;101:2309–2316.
15. Shindo T, Kurihara Y, Nishimatsu H, Moriyama N, Kakoki M, Wang Y, Imai Y, Ebihara A, Kuwaki T, Ju KH, Minamino N, Kangawa K, Ishikawa T, Fukuda M, Akimoto Y, Kawakami H, Imai T, Morita H, Yazaki Y, Nagai R, Hirata Y, Kurihara H. Vascular abnormalities and elevated blood pressure in mice lacking adrenomedullin gene. *Circulation.* 2001;104:1964–1971.
16. Chintala MS, Chiu PJ, Vemulapalli S, Watkins RW, Sybertz EJ. Inhibition of endothelial derived relaxing factor (EDRF) aggravates ischemic acute renal failure in anesthetized rats. *Naunyn Schmiedebergs Arch Pharmacol.* 1993;348:305–310.
17. Conger J, Robinette J, Villar A, Raij L, Shultz P. Increased nitric oxide synthase activity despite lack of response to endothelium-dependent vasodilators in postischemic acute renal failure in rats. *J Clin Invest.* 1995; 96:631–638.
18. Noiri E, Peresleni T, Miller F, Goligorsky MS. In vivo targeting of inducible NO synthase with oligodeoxynucleotides protects rat kidney against ischemia. *J Clin Invest.* 1996;97:2377–2383.
19. Kakoki M, Hirata Y, Hayakawa H, Suzuki E, Nagata D, Tojo A, Nishimatsu H, Nakanishi N, Hattori Y, Kikuchi K, Nagano T, Omata M. Effects of tetrahydrobiopterin on endothelial dysfunction in rats with ischemic acute renal failure. *J Am Soc Nephrol.* 2000;11:301–309.
20. Ichiki Y, Kitamura K, Kangawa K, Kawamoto M, Matsuo H, Eto T. Distribution and characterization of immunoreactive adrenomedullin in human tissue and plasma. *FEBS Lett.* 1994;338:6–10.
21. Hayakawa H, Hirata Y, Suzuki E, Sugimoto T, Matsuoka H, Kikuchi K, Nagano T, Hirobe M. Mechanisms for altered endothelium-dependent vasorelaxation in isolated kidneys from experimental hypertensive rats. *Am J Physiol.* 1993;264:H1535–H1541.
22. Hirata Y, Hayakawa H, Suzuki E, Kimura K, Kikuchi K, Nagano T, Hirobe M, Omata M. Direct measurements of endothelium-derived nitric oxide release by stimulation of endothelin receptors in rat kidney and its alteration in salt-induced hypertension. *Circulation.* 1995;91:1229–1235.
23. Saeki T, Adachi H, Takase Y, Yoshitake S, Souda S, Saito I. A selective type V phosphodiesterase inhibitor, E4021, dilates porcine large coronary artery. *J Pharmacol Exp Ther.* 1995;272:825–831.
24. Solez K, Morel-Maroger L, Sraer JD. The morphology of "acute tubular necrosis" in man: analysis of 57 renal biopsies and a comparison with the glycerol model. *Medicine.* 1979;58:362–376.
25. Kurihara Y, Kurihara H, Suzuki H, Kodama T, Maemura K, Nagai R, Oda H, Kuwaki T, Cao WH, Kamada N, et al. Elevated blood pressure and craniofacial abnormalities in mice deficient in endothelin-1. *Nature.* 1994;368:703–710.
26. Huang PL, Huang Z, Mashimo H, Bloch KD, Moskowitz MA, Bevan JA, Fishman MC. Hypertension in mice lacking the gene for endothelial nitric oxide synthase. *Nature.* 1995;377:239–242.
27. Nuki C, Kawasaki H, Kitamura K, Takenaga M, Kangawa K, Eto T, Wada A. Vasodilator effect of adrenomedullin and calcitonin gene-related peptide receptors in rat mesenteric vascular beds. *Biochem Biophys Res Commun.* 1993;196:245–251.
28. Watanabe TX, Itahara Y, Inui T, Yoshizawa-Kumagaye K, Nakajima K, Sakakibara S. Vasopressor activities of N-terminal fragments of adrenomedullin in anesthetized rat. *Biochem Biophys Res Commun.* 1996; 219:59–63.
29. Shesely EG, Maeda N, Kim HS, Desai KM, Krege JH, Laubach VE, Sherman PA, Sessa WC, Smithies O. Elevated blood pressures in mice lacking endothelial nitric oxide synthase. *Proc Natl Acad Sci U S A.* 1996;93:13176–13181.
30. Fagan KA, Fouty BW, Tyler RC, Morris KG Jr, Hepler LK, Sato K, LeCras TD, Abman SH, Weinberger HD, Huang PL, McMurtry IF, Rodman DM. The pulmonary circulation of homozygous or heterozygous eNOS-null mice is hyperresponsive to mild hypoxia. *J Clin Invest.* 1999; 103:291–299.
31. Hirata Y, Mitaka C, Sato K, Nagura T, Tsunoda Y, Amaha K, Marumo F. Increased circulating adrenomedullin, a novel vasodilatory peptide, in sepsis. *J Clin Endocrinol Metab.* 1996;81:1449–1453.
32. Nishio K, Akai Y, Murao Y, Doi N, Ueda S, Tabuse H, Miyamoto S, Dohi K, Minamino N, Shoji H, Kitamura K, Kangawa K, Matsuo H. Increased plasma concentrations of adrenomedullin correlate with relaxation of vascular tone in patients with septic shock. *Crit Care Med.* 1997;25:953–957.
33. Ohashi Y, Kawashima S, Hirata K, Yamashita T, Ishida T, Inoue N, Sakoda T, Kurihara H, Yazaki Y, Yokoyama M. Hypotension and reduced nitric oxide-elicited vasorelaxation in transgenic mice overexpressing endothelial nitric oxide synthase. *J Clin Invest.* 1998;102: 2061–2071.
34. Yamashita T, Kawashima S, Ohashi Y, Ozaki M, Rikitake Y, Inoue N, Hirata K, Akita H, Yokoyama M. Mechanisms of reduced nitric oxide/cGMP-mediated vasorelaxation in transgenic mice overexpressing endothelial nitric oxide synthase. *Hypertension.* 2000;36:97–102.
35. Conger JD, Robinette JB, Schrier RW. Smooth muscle calcium and endothelium-derived relaxing factor in the abnormal vascular responses of acute renal failure. *J Clin Invest.* 1988;82:532–537.
36. Sata M, Kakoki M, Nagata D, Nishimatsu H, Suzuki E, Aoyagi T, Sugiura S, Kojima H, Nagano T, Kangawa K, Matsuo H, Omata M, Nagai R, Hirata Y. Adrenomedullin and nitric oxide inhibit human endothelial cell apoptosis via a cyclic GMP-independent mechanism. *Hypertension.* 2000;36:83–88.
37. Nava E, Llinas MT, Gonzalez JD, Salazar FJ. Nitric oxide synthase activity in renal cortex and medulla of normotensive and spontaneously hypertensive rats. *Am J Hypertens.* 1996;9:1236–1239.
38. Hayakawa H, Raij L. Nitric oxide synthase activity and renal injury in genetic hypertension. *Hypertension.* 1998;31:266–270.
39. Wu F, Park F, Cowley AW Jr, Mattson DL. Quantification of nitric oxide synthase activity in microdissected segments of the rat kidney. *Am J Physiol.* 1999;276:F874–F881.
40. Szentivanyi M Jr, Zou AP, Maeda CY, Mattson DL, Cowley AW Jr. Increase in renal medullary nitric oxide synthase activity protects from norepinephrine-induced hypertension. *Hypertension.* 2000;35:418–423.

J Mol Med (2002) 80:105–116
DOI 10.1007/s00109-001-0284-4

ORIGINAL ARTICLE

T. Shindo · H. Kurihara · K. Maemura · Y. Kurihara
O. Ueda · H. Suzuki · T. Kuwaki · K.-H. Ju · Y. Wang
A. Ebihara · H. Nishimatsu · N. Moriyama
M. Fukuda · Y. Akimoto · H. Hirano · H. Morita
M. Kumada · Y. Yazaki · R. Nagai · K. Kimura

Renal damage and salt-dependent hypertension in aged transgenic mice overexpressing endothelin-1

Received: 28 June 2001 / Accepted: 28 August 2001 / Published online: 8 November 2001

H. Kurihara (✉)
Division of Integrative Cell Biology, Department of Embryogenesis, Institute of Molecular Embryology and Genetics, Kumamoto University, 2-2-1 Honjo, Kumamoto 860–0811, Japan
e-mail: kurihara@kaiju.medic.kumamoto-u.ac.jp
Tel.: +81-96-3736615, Fax: +81-96-3736618

T. Shindo · K. Maemura · Y. Kurihara · Y. Wang · H. Morita · R. Nagai
Department of Cardiovascular Medicine, Graduate School of Medicine, University of Tokyo, Tokyo, Japan

H. Kurihara
Department of Embryogenesis, Institute of Molecular Embryology and Genetics, Kumamoto University, Kumamoto, Japan

O. Ueda
Chugai Pharmaceutical Corporation, Shizuoka, Japan

H. Suzuki
National Research Center for Protozoan Diseases, Obihiro University of Agriculture and Veterinary Medicine, Obihiro, Japan

T. Kuwaki
Department of Physiology, School of Medicine, Chiba University, Chiba, Japan

K.-H. Ju
Department of Physiology, Graduate School of Medicine, University of Tokyo, Tokyo, Japan

A. Ebihara
The Institute for Adult Disease Asahi Life Foundation, Tokyo, Japan

H. Nishimatsu · N. Moriyama
Department of Urology, Graduate School of Medicine, University of Tokyo, Tokyo, Japan

M. Fukuda · Y. Akimoto · H. Hirano
Department of Anatomy, Kyorin University, Tokyo, Japan

M. Kumada
St Luke's College of Nursing, Tokyo, Japan

Y. Yazaki
The Hospital International Medical Center of Japan, Tokyo, Japan

K. Kimura
Department of Nephrology and Endocrinology, Graduate School of Medicine, University of Tokyo, Tokyo, Japan

K. Kimura
Division of Nephrology and Hypertension, Department of Internal Medicine, St. Marianna University School of Medicine, Kanagawa, Japan

J Mol Med 2002 Feb;80(2):69–70

Comment on:
- J Mol Med. 2002 Feb;80(2):105–16.

Endothelin, nephropathy, and blood pressure.

Luft FC.

Franz-Volhard-Klinik, Humboldt University of Berlin, Wiltbergstrasse 50, 13125 Berlin-Buch, Germany. luft@fvk-berlin.de

TAKAYUKI SHINDO received his PhD in cardiology from the University of Tokyo, Tokyo, Japan. He is presently a Research Fellow of the Organization for Drug ADR Relief, R&D Promotion and Product Review of Japan. His research interests include the pathophysiological assessment of cardiovascular disease by the mice gene-engineering approach.

KENJIRO KIMURA received his PhD in nephrology from the University of Tokyo, Tokyo, Japan. He is presently Professor of Medicine, Director of Division of Nephrology and Hypertension at St. Marianna University School of Medicine. His research interests include the pathogenesis of renal disease and the mechanisms for progression of renal diseases.

Abstract The recent development of endothelin-1 (ET-1) antagonists and their potential use in the treatment of human disease raises questions as to the role of ET-1 in the pathophysiology of such cardiovascular ailments as hypertension, heart failure, renal failure and atherosclerosis. It is still unclear, for example, whether activation of an endogenous ET-1 system is itself the primary cause of any of these ailments. In that context, the phenotypic manifestations of chronic ET-1 overproduction may provide clues about the tissues and systems affected by ET-1. We therefore established two lines of transgenic mice overexpressing the ET-1 gene under the direction of its own promoter. These mice exhibited low body weight, diminished fur density and two- to fourfold increases in

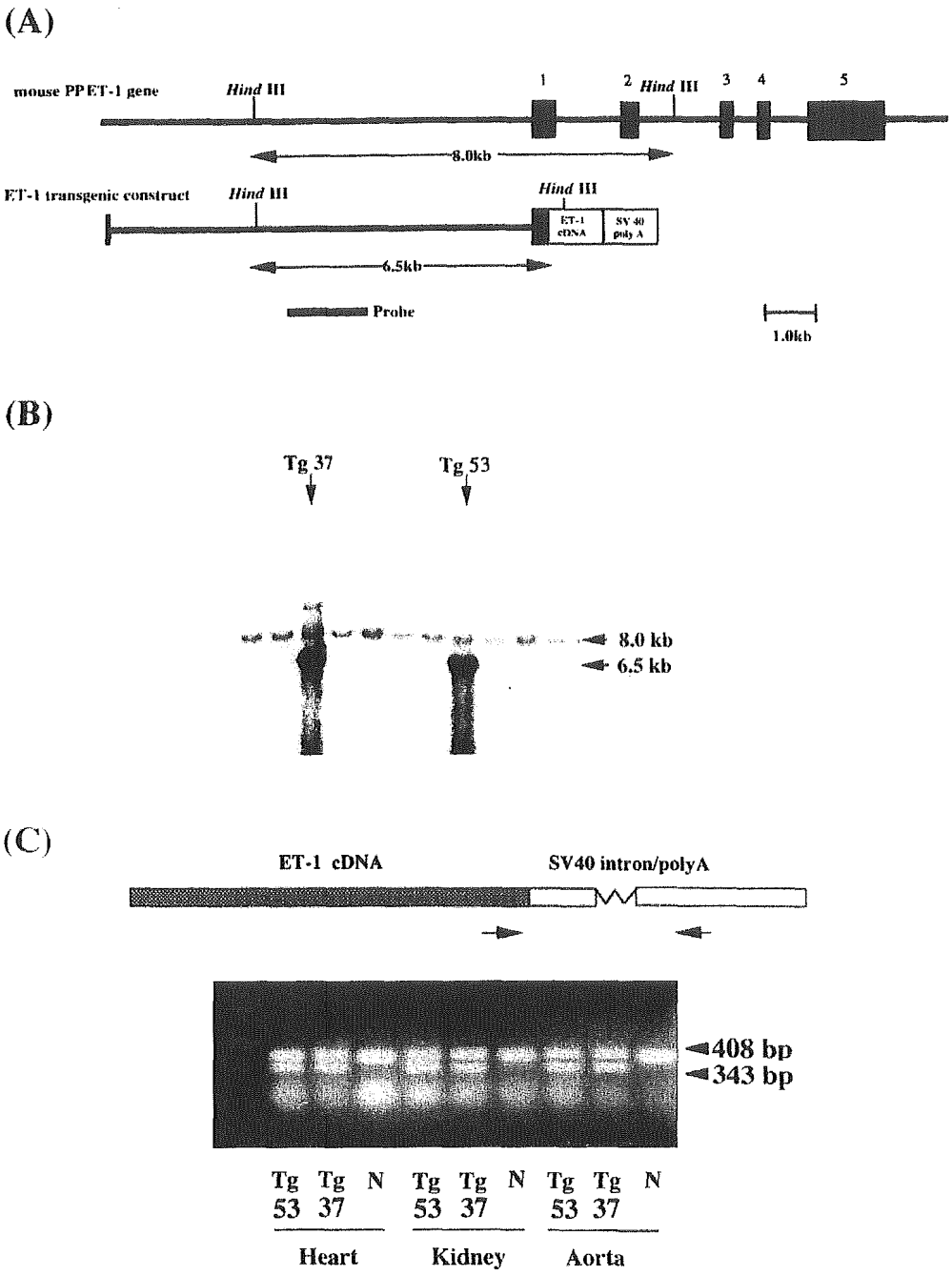

Fig. 1 **A** Structure and restriction maps of the mouse PPET-1 gene and the transgenic construct. *Filled boxes* represent exons 1–5 of the PPET-1 gene. The length of the *Hind*III-digested diagnostic DNA fragments and the probe for Southern blot analysis are shown. **B** Representative genomic Southern blot analysis. The 8.0-kb and 6.5-kb *Hind*III bands reflect the authentic PPET-1 gene and the transgene, respectively. **C** Representative RT-PCR demonstrating expression of the ET-1 transgene. *Arrows* in the figure indicate the primers for RT-PCR. In Tg 37 and Tg 53, the amplified products derived from the integrated transgene could be discriminated by a 65-bp difference caused by the SV40 intron, whereas no such product was detected in the nonexpresser (*N*). **D** Plasma and tissue endothelin-1 (*ET-1*) concentrations in ET-1 transgenic and wild-type mice. $^{\#}P<0.05$, $^{*}P<0.01$ versus wild-type mice. **E**, **F** Representative sections showing immunohistochemical staining for ET-1 in the kidneys of wild-type (**E**) and Tg 53 transgenic (**F**) mice. Specific staining for ET-1 was detected in the glomeruli (*g*) and vascular endothelium (*a*) of transgenic mice, whereas wild-type kidneys showed only faint staining in glomeruli. *Scale bars* in **E** and **F**, 100 μm

the ET-1 levels measured in plasma, heart, kidney and aorta. There were no apparent histological abnormalities in the visceral organs of young (8 weeks old) transgenic mice, nor was their blood pressure elevated. In aged (12 months old) transgenic mice, however, renal manifestations, including prominent interstitial fibrosis, renal cysts, glomerulosclerosis and narrowing of arterioles, were detected. These pathological changes were accompanied by decreased creatinine clearance, elevated urinary protein excretion and salt-dependent hypertension. It thus appears that mild, chronic overproduction of ET-1 does not primarily cause hypertension but triggers damaging changes in the kidney which lead to the susceptibility to salt-induced hypertension.

Keywords Aging · Blood pressure · Endothelin · Hypertension · Renal function

Since its initial characterization as an endothelial cell-derived vasoconstrictor a decade ago [1], the peptide endothelin-1 (ET-1) has been found to possess a diverse set of biological activities, including effects on cell proliferation and hypertrophy, regulation of hormone release and modulation of central nervous system activity [2, 3, 4]. In addition, elevated plasma ET-1 has been associated with such cardiovascular diseases as hypertension [5], heart failure [6], renal failure [7] and atherosclerosis [8], thus implicating it in the regulation of cardiovascular ho-

Fig. 1D–F

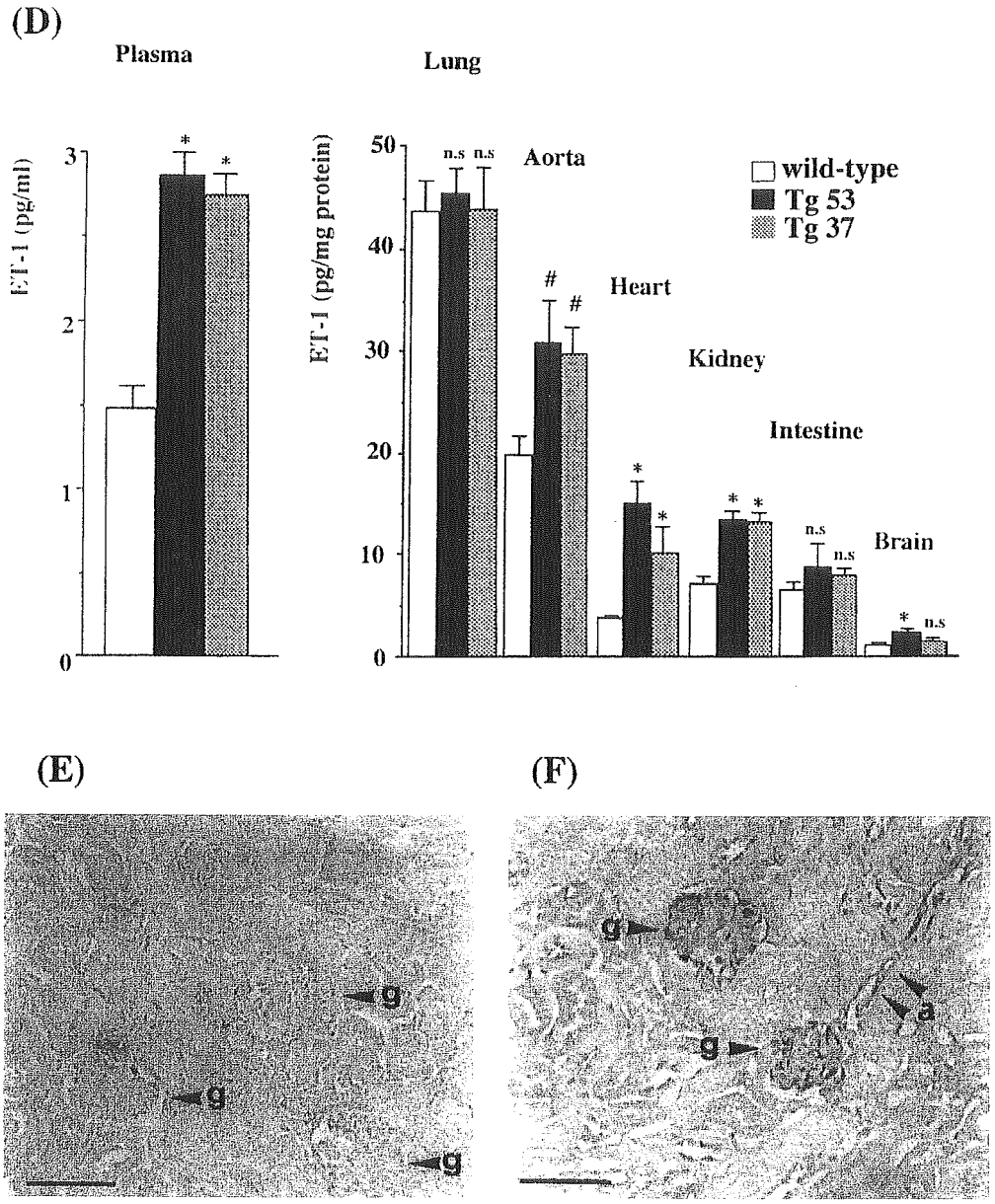

meostasis. The recent development of selective ET antagonists and their potential use in the treatment of cardiovascular disease raises questions as to the role of ET-1 in the disease process [9]. It is still unclear whether activation of an endogenous ET-1system could be the primary cause of any of the aforementioned ailments. For example, patients with essential hypertension had elevated plasma ET-1 levels, but there was no significant correlation between the plasma ET-1 level and systolic or diastolic blood pressure (BP) in these patients [10].

Animal models in which ET-1 production is chronically increased should serve as a useful tool with which to obtain a better understanding of the function of ET-1 in cardiovascular pathophysiology. In particular, the use of transgenic mice overexpressing ET-1 enables us to focus on the effects of chronically elevated ET-1 on selected organs, so as to better understand the specific benefits of anti-ET therapy. Based on our previous work showing the utility of the murine (prepro)endothelin-1 (PPET-1) gene 5′-flanking region for this purpose [11], we generated transgenic mice using a DNA construct in which the promoter region was inserted upstream of murine ET-1 cDNA and analyzed their phenotype with special reference to BP regulation and organ damage.

Materials and methods

Transgenic construct

A mouse ET-1 cDNA fragment encompassing the open reading frame was obtained from mouse lung cDNA by reverse transcription (RT) polymerase chain reaction (PCR) using primers deduced from the previously reported sequence [12]. The amplified 1.0-kb fragment was cloned into pCRII vector using a TA cloning kit (Invitrogen), and *Not*I sites were placed at either end of the fragment

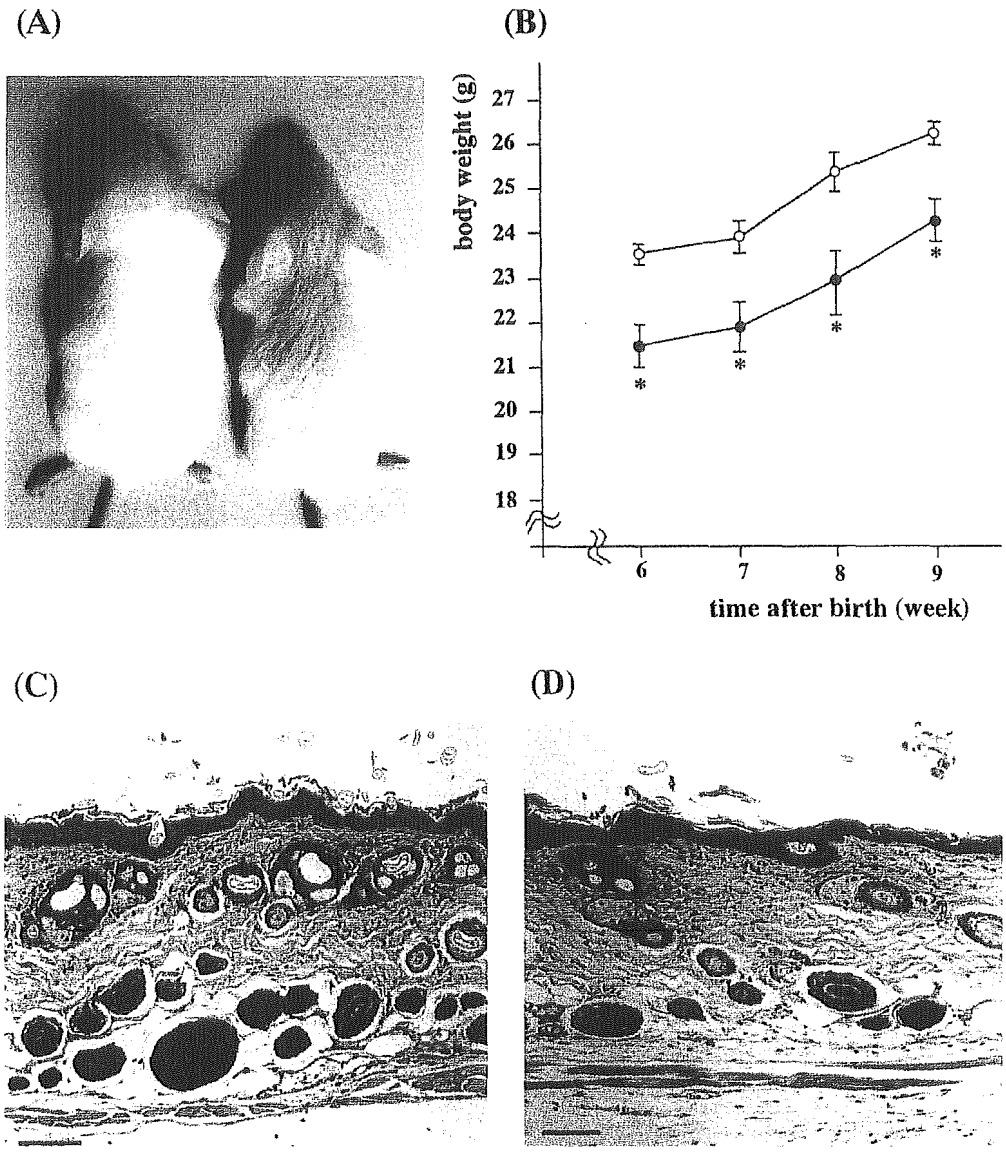

Fig. 2 **A** Representative specimens of 10-week-old transgenic (*right*) and wild-type (*left*) mice. Note the smaller size of the transgenic mouse and the courser, sparser fur. **B** Time-dependent increases in body weight in transgenic (*closed circles*) and wild-type (*open circles*) mice (n=10 for each). $^{*}P<0.01$ versus wild-type mice. **C**, **D** Representative skin sections from wild-type (**C**) and transgenic (**D**) mice. *Scale bars* in **C** and **D**, 200 μm

using synthetic linkers. The resultant *Not*I cassette was then inserted into a plasmid containing a 9.2-kb fragment of the murine PPET-1 gene 5′-flanking region, including a 131-bp sequence from exon 1 and a 0.7-kb SV40-derived sequence with an intron and an additional poly-A signal [11]. The final construct is illustrated in Fig. 1A.

Generation and identification of transgenic mice

The investigation conforms with the *Guide for the Care and Use of Laboratory Animals* published by the US National Institutes of Health (NIH Publication No. 85–23, revised 1996).

The PPET-1 5′-flanking promoter region-ET-1 cDNA construct was liberated from the vector by *Xho*I digestion and then purified using agarose gel electrophoresis and a Geneclean kit (BIO101). The purified DNA was dissolved in 5 mM Tris (pH 7.4) plus 0.1 mM EDTA before pronuclear injection into donor eggs prepared from FvB mice. The final injection concentration was calculated to be 500 copies/pl. Microinjected eggs were transferred to the oviducts of pseudopregnant ICR foster mothers and allowed to develop to term. Founder mice were identified by standard Southern blot analysis of tail DNA using a 2-kb fragment of the PPET-1 promoter gene sequence as a probe. When the genomic DNA was digested with *Hin*dIII, a 6.5-kb transgene band, distinguishable from the 8.0-kb authentic gene band, was observed.

For RT-PCR, the sense primer (5′-TAGGGAGTGTTCGTGTCTGACTCA-3′) was chosen within the mouse ET-1 cDNA sequence. The antisense primer (5′-AGATGGCATTTCTTCTGAGC-3′) was chosen within an SV40 intron/poly-A additional signal sequence. These primers were chosen to be situated upstream and downstream of the SV40 intron sequence, respectively. In transgenic mice that showed the transcription of the transgene, the RT-PCR product from the mRNA was 65 bp shorter because of the splicing at the SV40 intron site (Fig. 1C).

Endothelin-1 measurement

ET-1 was extracted from tissue and plasma as described previously [13, 14]. Immunoreactive ET-1 was measured using a commercial endothelin enzyme immunoassay kit according to the manufacturer's (Wako) instructions.

Immunohistochemistry

Samples embedded in OCT compound were cut into 8-μm frozen sections on a cryostat. Slide-mounted tissue sections were washed

with PBS, treated with 0.3% H_2O_2 in methanol, preincubated with goat nonimmune serum, and then incubated for 16 h at 4°C with rabbit anti-rat polyclonal ET-1 antibody. Thereafter, the sections were incubated for 60 min at 37°C with biotinylated goat anti-rabbit IgG, washed, treated with avidin-biotinylated horseradish peroxidase complex (Vectastain ABC kit, Vector), and developed in 0.004% H_2O_2 and 0.02% diaminobenzidine tetrahydrochloride. Samples labeled with preimmune serum instead of the primary antibody served as a negative control.

Electron microscopy

Small samples of the specimens were fixed with glutaraldehyde and osmium tetroxide, embedded in Epon (Epok) 812 (Oken Shoji, Tokyo, Japan), cut into 0.1-μm sections, double-stained with uranyl acetate or phosphotungstic acid and lead citrate, and examined with an electron microscope.

Vascular casting and scanning electron microscopy

Mice were anesthetized with sodium pentobarbital, and the aorta was cannulated via the left ventricle and perfused with 100 ml PBS containing 0.1% heparin. The lower portion of the descending aorta was then cross-clamped, and perfusion fixation was carried out for 5 min using 100 ml of 2.5% glutaraldehyde at 37°C. Thereafter, 10 ml of casting resin (Mercox CL2B, Dainippon-ink and Chemical, Tokyo, Japan), mixed with a polymerizer in a 1.7% volume ratio, was infused under hand pressure and allowed to polymerize for 30 min at room temperature. The kidneys were then removed and immersed in a 20% KOH solution at room temperature for 1–2 days to corrode the tissue. After washing in water, the vascular casts were dried in an incubator at 40°C. Areas of the cast corresponding to the cortex were then cut with a razor blade into small pieces suitable for observation, gold-coated with an ion sputter and observed under a scanning electron microscope (JSM-5600LV, JEOL, Tokyo, Japan) using an accelerating voltage of 15 kV.

Measurement of blood pressure

Male transgenic mice heterozygous for the ET-1 transgene and their wild-type littermates were maintained on normal mouse chow containing 1% NaCl. Using a ventilator (Harvard rodent ventilator model 683), the mice were then halothane anesthetized, and their femoral arteries were cannulated with polyethylene tubing (I.D., 0.28 mm; O.D., 0.61 mm). To measure BP, the cannula was connected a pressure transducer (TP-400T, Nihon-Kohden), and arterial pressure was determined every 2.5 s using a peak detector (AP-611G, Nihon-Kohden). Pulsatile BP was monitored in this way for more than 5 h while the mice were conscious and unrestrained within a quiet environment. BP data were stored on tape along with the corresponding heart rates, which were computed using a tachometer (AT-601G, Nihon-Kohden). The data were then input to a computer, and the mean values for each variable were calculated for 2-h segments composed of 2880 sample points each.

To investigate the salt sensitivity of the mice, diet containing a high (8%) amount of sodium was provided for up to 3 weeks. This dose could cause BP elevation in Dahl salt-sensitive rats within 3 weeks [15]. The systolic BP was measured by a programmable sphygmomanometer connected to a cuff probe for mice (98A, Softron). Unanesthetized mice were introduced into a small holder and placed within a thermostatically controlled warming drum and maintained at 37°C during the measurements.

Evaluation of renal function

All mice were housed in individual metabolic cages, and a series of 24-h urine sample collections were made for 5 days. In each mouse, we used the urine samples from days 3–5 and calculated the mean urine volume and concentrations of urinary protein and creatinine. After 5 days, blood was drawn to measure serum creatinine. Creatinine clearance was used as an index of glomerular filtration rate and was calculated using the formula: creatinine clearance=urinary creatinine × urine volume/serum creatinine.

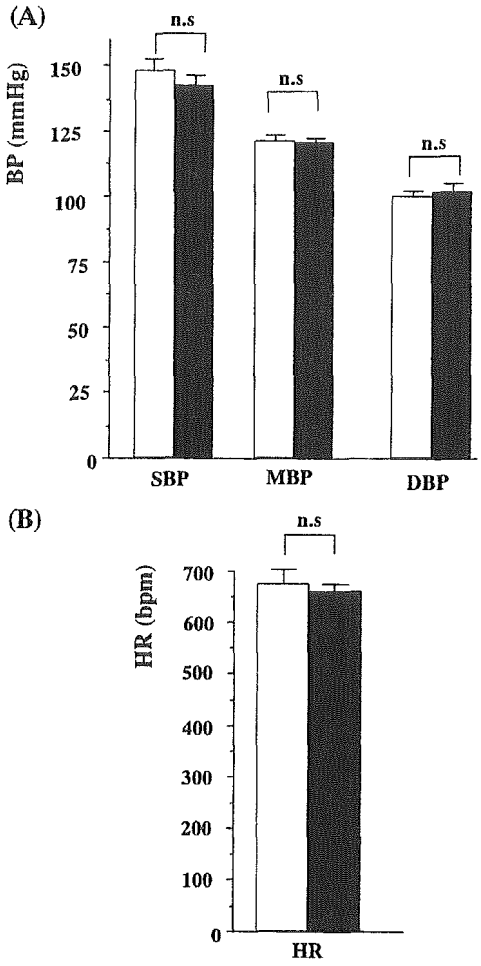

Fig. 3 Comparison of basal arterial blood pressure (BP) (**A**) and heart rates (**B**) in conscious, unrestrained ET-1 transgenic mice (n=8, *filled columns*) and their wild-type littermates (n=10, *open column*). (*DBP* Diastolic blood pressure, *HR* heart rate, *MBP* mean blood pressure, *SBP* systolic blood pressure)

Statistical analysis

Data are expressed as means ±SEM. Student's t-test was used to evaluate differences between groups. Values of $P<0.05$ were considered significant.

Results

Establishment and characterization of ET-1 transgenic mice

Microinjection of the transgenic construct into fertilized mouse eggs gave rise to 50 live-born offspring. Among them, eight were founders carrying the transgene, which was identified by Southern blot analysis of the genomic DNA (Fig. 1B). Amplification of the products by RT-

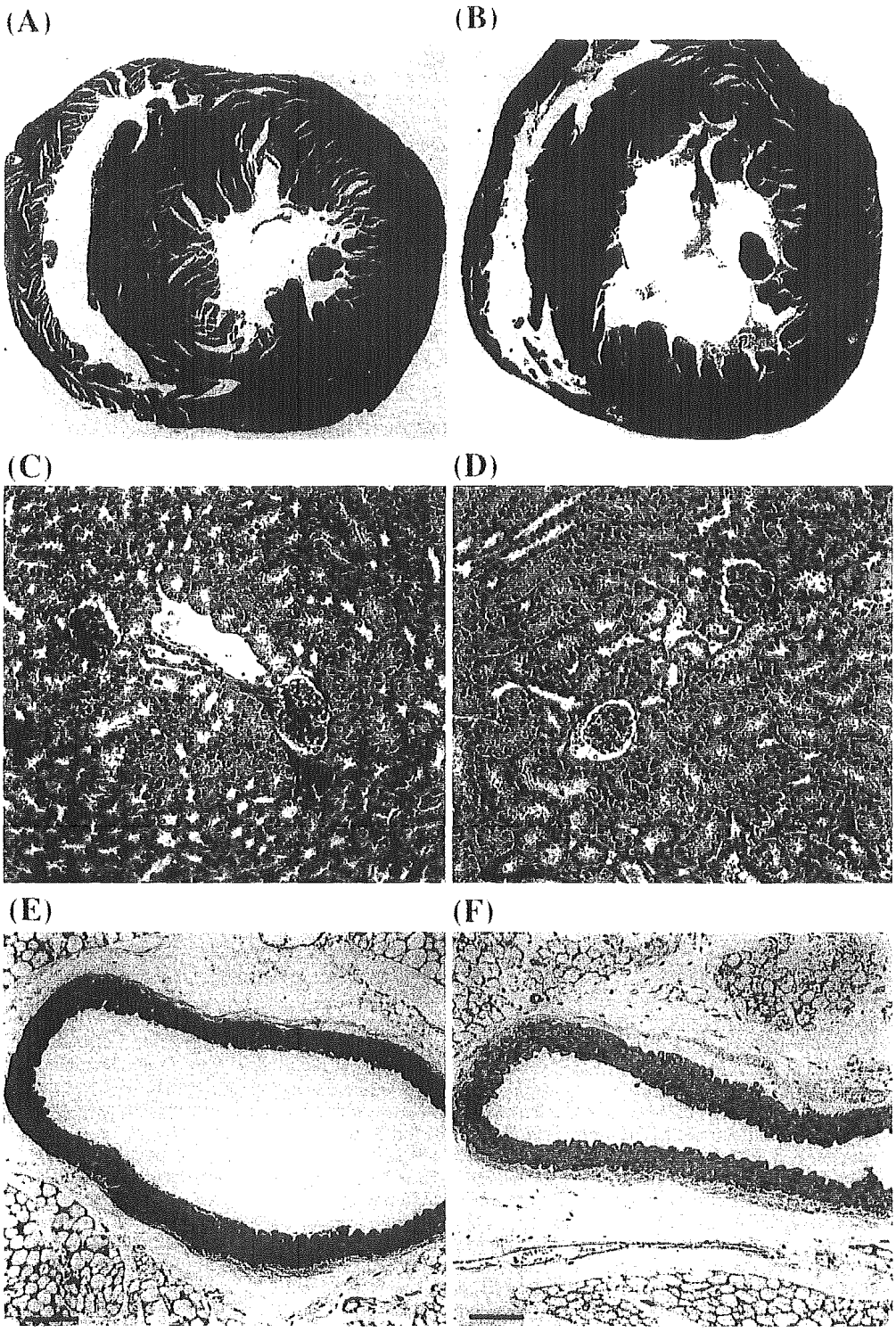

Fig. 4 Representative sections showing histological characteristics of the heart (**A**, **B**), kidney (**C**, **D**) and aorta (**E**, **F**) from 8- to 10-week-old wild-type (**A**, **C**, **E**) and ET-1 transgenic (**B**, **D**, **F**) mice. *Scale bars* in **C** and **D**, 100 μm; **E** and **F**, 200 μm

PCR confirmed that two lines transcribed the transgene (Fig. 1C). The two lines, designated Tg 53 and Tg 37, carried ten and nine copies of the transgene, respectively. As compared to their wild-type littermates, ET-1 concentrations in the plasma, aorta, heart, kidney and intestine were elevated about twofold in both lines (Fig. 1D). The effect of ET-1 overexpression was assessed mainly using the Tg 53 line in the latter studies, because the expression levels in each organ were almost equal and histological changes were identical between these lines.

Localization of ET-1 expression in the kidney was analyzed immunohistochemically. The glomeruli in kidney samples from transgenic mice were intensively labeled by anti-ET-1 antibody (Fig. 1F), whereas the signal from kidneys of wild-type mice was small (Fig. 1E). This pat-

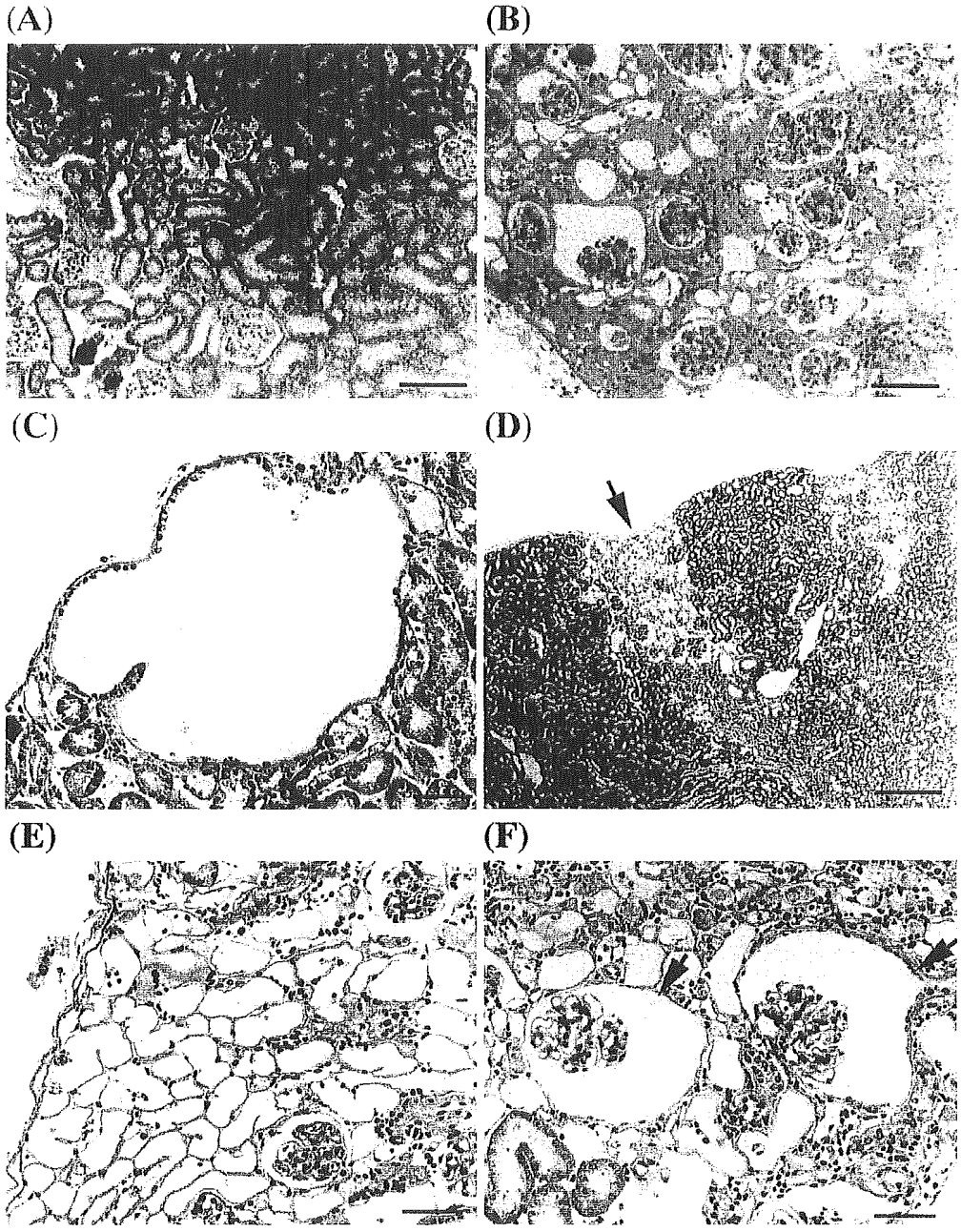

Fig. 5 Kidney sections from 12-month-old wild-type (**A**) and transgenic (**B–F**) mice. Interstitial fibrosis in transgenic mice was made apparent by staining blue with Masson Trichrome stain (**B**). **C–F** Cystic lesions detected in the kidney of transgenic mice. **C** Enlarged renal cyst located at the surface of the kidney. **D, E** Focal assembly of small cysts. **F** Glomerular cysts; note the abnormal dilatation of Bowman's capsule (*arrows*) and the shrinkage of the glomerular tuft. **G–J** Glomeruli from transgenic (**H, J**) and wild-type (**G, I**) mice, **G, H** PAS stain, **I, J** immunohistochemistry of fibronectin. Glomeruli of transgenic mice exhibited increased numbers of mesangial cells, the accumulation of mesangial matrix and thickening of the basement membrane (**H**). Immunohistochemistry of fibronectin revealed strong positive staining in the mesangial area in transgenic mice (**J**). *Scale bars* in **A** and **B**, 100 μm; **C, E** and **F** 50 μm; **D** 20 μm; and **G–J** 200 μm. **K** Comparison of glomerular planar area in wild-type (*open column*) and transgenic mice (*filled column*). $^{*}P<0.01$ versus wild-type mice

tern of ET-1 expression in the kidney was almost identical to that in PPET-1-luciferase transgenic mice exhibiting vasculature-selective transgene expression driven by the same promoter [11].

Appearance of ET-1 transgenic mice

Transgenic mice weighed about 90% as much as their wild-type littermates at every stage examined (Fig. 2A, B). In fact, the reduced body weight was already apparent at birth, when the weight of the fat between the scapulae was also only about 90% that of the wild-type mice. In addition, the fur of the transgenic mice was coarse, and the number of follicles present in skin sections was diminished (Fig. 2C, D). In all other respects, the appearance, behavior and fertility of the transgenic lines were unaffected.

Measurement of blood pressure, heart rate and creatinine clearance in young mice

When the arterial BP was assessed in 8- to 10-week-old, conscious, unrestrained mice, no significant differences between wild-type (n=10) and transgenic (n=8) mice were found (mean BP, 121±1 mmHg versus 120±2 mmHg; heart rate, 674±26 bpm versus